

87. R. A. Whiteside, M. J. Frisch and J. A. Pople, *The Carnegie-Mellon Quantum Chemistry Archive* (3rd Ed, Carnegie-Mellon University, Pittsburgh, 1983) and associated computer database.
88. K. Ohno and K. Morokuma, *Quantum Chemistry Literature Data Base* (Elsevier, Amsterdam, 1982; yearly supplements published in special issues of the journal *Theochem*) and associated computer database.
89. F. H. Allen, O. Kennard and R. Taylor, *Acc. Chem. Res.* 16, 146 (1983) and associated Cambridge Structural Database.
90. U. Burkhardt and N. L. Allinger, *Molecular Mechanics*, ACS monograph no. 177, (American Chemical Society, Washington, DC, 1982).
91. H. B. Schlegel, *Theoret. Chim. Acta* 66, 333 (1984).

Note: The surfaces in Figs. 1, 4-6 are of the form $E = \sum_i a_i \exp(-b_i(x - c_i)^2 - d_i(y - e_i)^2)$. For Figs. 1 and 4, $a = (1.7, 1.7, 0.8, 0.8, -1, -1, -0.25, -0.25, -0.5)$, $b = (1.5, 1.5, 4, 4, 14, 14, 4, 4, 4)$, $c = (-0.25, 1.75, -0.1, 1.6, 0.35, 1.15, -0.75, 2.25, 0.75)$, $d = (4, 4, 4, 4, 4, 4, 4, 4)$, $e = (0.5, 0.5, -0.95, -0.95, -0.75, -0.75, -0.75, 1.2)$. For Figs. 5 and 6, $a = (1.7, 1.7, 0.8, 0.8, -1, -0.25, -0.25, -0.5)$, $b = (1.5, 1.5, 4, 4, 8, 2, 2, 4)$, $c = (-0.25, 1.75, -0.1, 1.6, 0.55, -0.75, 2.25, 0.75)$, $d = (4, 4, 4, 4, 2, 4, 4, 4)$, $e = (0.5, 0.5, -0.95, -0.75, -0.75, -0.75, 1.2)$. Note that there are other, lower energy saddle points outside of the range $x = \pm 1$, $y = \pm 1$. For Fig. 2, the adiabatic surfaces, $S_{\pm} = [E_+ + E_- \pm \sqrt{(E_+ - E_-)^2 + 4h^2}] / 2$, are obtained by solving the secular equation for two diabatic surfaces $E_{\pm} = (x \pm 2)^2 + y^2$ interacting via a matrix element h ; in (a) $h^2 = 0$, in (b) $h^2 = 16y^2$, and in (c) $h^2 = 16y^2 + 1$.

CHAPTER 9

THE INCORPORATION OF MODERN ELECTRONIC STRUCTURE METHODS IN ELECTRON-MOLECULE COLLISION PROBLEMS: VARIATIONAL CALCULATIONS USING THE COMPLEX KOHN METHOD

T. N. Rescigno and B. H. Lengsfeld III

*Physics Department, Lawrence Livermore National Laboratory
University of California, Livermore, California 94550, USA*

C. W. McCurdy

*National Energy Research Supercomputer Center
Lawrence Livermore National Laboratory
University of California, Livermore, California 94550, USA*

Contents

1. Introduction	502
1.1. Background	503
1.2. Electronic Structure and Electron Scattering	504
2. Theoretical Formulation	506
2.1. Variational Theory	506
2.2. Continuum Basis Functions	509
2.3. Trial Wave Function for Multichannel Scattering	511
2.4. P- and Q-Space Partitioning	513
2.5. Separable Expansions	519
2.6. Adaptive Quadrature	522
2.7. Cross-Sections	526
2.8. New Technology for Bound-Free Integrals	527

3. Aspects of the Close-Coupling Method	534
3.1. The Close-Coupling Plus Correlation Method	534
3.2. The Multiconfiguration Close-Coupling Method	535
3.3. Intermediate Energy Scattering	540
4. Long-Range Interactions	542
4.1. Dipole Interactions	543
5. Applications	548
5.1. Polarized-SCF Studies (CH_4 , SiH_4 , C_2H_4 , C_2H_6)	548
5.2. Polar Molecules (H_2O , NH_3 and H_2S)	556
5.3. Target Correlation Effects — the Li_2 Example	562
5.4. Electronic Excitation (H_2 , F_2 , CH_2O , C_2H_4)	568
6. Future Directions	582
Acknowledgments	583
References	583

1. Introduction

Low-energy electron-molecule collisions are the basis of a wide range of important physical processes. A quantitative understanding of these processes is needed in such diverse areas as advanced laser development, pollution control, the design of high-speed space re-entry vehicles, the manufacture of semiconductor devices, and plasma-driven chemical synthesis. For example, while the detailed modeling of a chemical vapor deposition process may require hundreds of reaction rates involving neutral radicals and ionic fragments, the rate determining steps which initiate this chemistry frequently involve the electron impact dissociation of a polyatomic molecule, such as SiH_4 or CH_4 , into neutral fragments.¹⁻³ The study of electron-molecule scattering is thus driven by the practical need to develop a better understanding of the physical processes that impact a number of important technologies.

Electron-polyatomic molecule collisions are also of fundamental theoretical importance. With many vibrational degrees of freedom and opportunities for interaction between excited electronic surfaces in several dimensions, these systems offer for study a body of physics that is far richer and more complex than that found with diatomic targets.

This chapter is concerned with an *ab initio* treatment of the fixed-nuclei electron-molecule scattering problem. Compared to the large number of high quality *ab initio* calculations that have been carried out on bound

molecular electronic states, *ab initio* calculations of electron-molecule collisions have been rather rare. Electron-molecule scattering is a complicated many-body problem in which electron correlation plays an important role, as it does in bound-state problems. It has the additional complications of a scattering problem, which necessitates the imposition of asymptotic boundary conditions on the wave function. The need to treat the incident plus target electrons as a system of indistinguishable particles leads to a scattering problem with non-local interactions that can be arbitrarily asymmetric. Moreover, accurate *ab initio* treatments that go beyond the simplest static-exchange level of approximation require an approach in which correlation among the target electrons, as well as correlation between the incident electron and those of the target molecule, are treated in a consistent manner. It is only within the last few years that *ab initio* electron-molecule calculations employing coupled electronic states and/or correlated target wave functions have begun to appear in the literature.

1.1. Background

Serious *ab initio* treatments of electron-molecule scattering had to await the advent of high-speed digital computers and there was considerable theoretical activity in this area during the 1970's. Much of this early work relied on techniques developed to treat electron-atom scattering; it was dominated by numerical solutions of the coupled equations generated by single-center expansion of the scattering wave function in Legendre polynomials.⁴⁻⁸ However, the difficulties of treating exchange and correlation for an asymmetric target were formidable with the single-center approach, and it soon became clear that, for significant progress to be made, more robust, "molecular-oriented" approaches would have to be developed. The ensuing decade of the 1980's saw the development of several hybrid approaches that combined numerical integration techniques with analytic basis set expansions. Most notable were the *R*-matrix⁹ and *T*-matrix methods,¹⁰ the *Schwinger* multichannel method¹¹ and the linear-algebraic approach.¹²

It is somewhat curious that algebraic variational methods based on the Kato identity,¹³ such as the Kohn variational method,¹⁴ which had been (and continue to be) used with much success in electron-atom problems,¹⁵ received virtually no attention in molecular applications during the decade of the 1970's and were not developed in this connection until the mid-1980's. Contributing to this neglect, no doubt, were the numerous problems asso-

ciated with the appearance of anomalous singularities in the K -matrices that made these techniques difficult to apply in large scale calculations.¹⁶ This latter problem, however, can be trivially avoided by formulating the variational problem with physical, traveling-wave (complex) boundary conditions, rather than real, standing-wave boundary conditions. This fact was originally used in nuclear physics by Mito and Kamimura,¹⁷ but went largely unnoticed until it was introduced into atomic and molecular physics by Miller and Jansen op de Haar in reactive heavy-particle scattering problems.¹⁸ The connection between Miller's original work, the Kohn method and Kapur-Peierls theory was pointed out by McCurdy, Rescigno and Schneider¹⁹ in 1987, and the complex Kohn method for electron-molecule scattering was developed over the ensuing few years. This development forms the subject of the present review.

Before closing this section, we should point out that there has also been considerable activity in electron-molecule scattering along completely different lines. Our focus here is on an *ab initio* treatment of the fixed-nuclei electronic problem. There has been a parallel development of model potential and semi-empirical approaches which have been very successful in reproducing a number of the features of *ab initio* theories with far less effort,²⁰ although the model potential approaches are effectively limited to electronically elastic problems. We should also point out that the fixed-nuclei electronic problem is only part of the full electron-molecule scattering picture. Much work centers on the nuclear motion problem, which is important in resonantly driven processes such as recombination and dissociative attachment,²¹ as well as near-threshold vibrational and rotational excitation.²² While meaningful cross-sections can frequently be extracted solely from fixed-nuclei calculations, in many other cases the fixed-nuclei electronic problem can provide the input necessary to solve the full problem, including the nuclear dynamics.²³

1.2. Electronic Structure and Electron Scattering

Theoretical treatments of electron-molecule collisions are complicated for a variety of reasons. For one, the problem is numerically complicated. Indeed, much of the literature in the field has focused on the development of robust numerical methods for treating the basic problem of scattering from a non-local, asymmetric potential. As we have said, several methods have been developed over the years that can adequately handle this problem, including the one on which we focus here, the complex Kohn method.

The technical aspects of the problem, unfortunately, have tended to obscure some of the more subtle aspects of electron-molecule collisions. The full wave function that describes the electron-molecule system represents a set of $N + 1$ indistinguishable particles that must be antisymmetric with respect to the interchange of their coordinates. Aside from the obvious difficulty of non-local potentials that arise from the antisymmetry of the wave function, there is the fact that electron correlation between the incident electron and the target electrons is inextricably connected to correlation among the target electrons. Now electron-target correlation is important. The position and width of shape resonances, for example, can be very sensitive to these effects. Other phenomena such as Ramsauer-Townsend minima — which are a ubiquitous feature in the low-energy cross-sections of many small polyatomic molecules — depend entirely on electron-target correlation for their existence. Consistency in the treatment of electron-target correlation and target electron correlation is essential in describing these phenomena. An analogous problem in bound-state theory is the calculation of electron affinities, which requires a careful balance of correlation effects in the N - and $(N + 1)$ -electron systems.

The primary difference between electronic structure and electron scattering is the need to account for asymptotic boundary conditions in the latter problem. In variational approaches, this need can be handled in one of two ways. One way is to use a formalism based on an integral equation approach that automatically builds in the correct asymptotic boundary conditions. The Schwinger multichannel technique¹¹ is such a method and is described in Chapter 22 in Part II of this volume. The alternative approach is to use a trial wave function that is augmented by an appropriate set of free functions. This allows us to use a formalism based on the Schrödinger equation which only requires Hamiltonian matrix elements. The form chosen for the trial wave function is intended to make the incorporation of bound-state quantum chemistry methodology as straightforward as possible.

The appearance of free functions in the trial wave function obviously leads to new types of integrals that have no analogue in bound-state problems. As we shall see, special techniques can be used to reduce the number of such integrals to a minimum and to efficiently handle those that are required. In a very real sense, the entire scattering calculation may be viewed as an elaborate electronic-structure calculation on the wave function of a transient negative ion which is connected to the asymptotic region by bound-free and free-free matrix elements.

2. Theoretical Formulation

2.1. Variational Theory

The basic concepts of the algebraic variational method and the derivation of the complex Kohn equations are most easily demonstrated for the case of single particle scattering by a spherically symmetric potential.²⁴ We will therefore consider this case in some detail before generalizing to the multi-channel case in the next section. Atomic units will be assumed throughout, unless otherwise stated. For the partial wave radial Schrödinger equation, we define the functional

$$L = \int_0^\infty u_\ell L u_\ell dr, \quad (1)$$

where

$$L = -\frac{1}{2} \frac{d^2}{dr^2} + \frac{\ell(\ell+1)}{2r^2} + V(r) - \frac{k^2}{2}, \quad (2)$$

and $V(r)$ is a short-ranged, spherically symmetric potential. (The formalism can easily be modified to handle Coulomb scattering.) The boundary conditions assumed for u_ℓ are

$$\begin{aligned} u_\ell(0) &= 0, \\ u_\ell(r) &\underset{r \rightarrow \infty}{\sim} F_\ell(kr) + \lambda G_\ell(kr), \end{aligned} \quad (3)$$

where F_ℓ and G_ℓ are two linearly independent solutions of the free particle radial Schrödinger equation with $V(r) = 0$.

If u_ℓ is an exact solution of the radial Schrödinger equation, then clearly L will vanish. Now consider how L changes when the exact u_ℓ is replaced by a trial solution u_ℓ^t satisfying the same boundary conditions specified by Eq. (3), that is, with

$$\delta u_\ell(r) \equiv u_\ell^t(r) - u_\ell(r), \quad (4)$$

and

$$\begin{aligned} \delta u_\ell(0) &= 0, \\ \delta u_\ell(r) &\underset{r \rightarrow \infty}{\sim} \delta \lambda G_\ell(r). \end{aligned} \quad (5)$$

The result is

$$\delta L = \int_0^\infty \delta u_\ell L u_\ell dr + \int_0^\infty u_\ell L \delta u_\ell dr + \int_0^\infty \delta u_\ell L \delta u_\ell dr. \quad (6)$$

Integrating the second term on the RHS of Eq. (6) by parts gives

$$\delta L = 2 \int_0^\infty \delta u_\ell L u_\ell dr - \frac{1}{2} [u_\ell(r) \delta u_\ell(r)' - \delta u_\ell(r) u_\ell(r)']_0^\infty + \int_0^\infty \delta u_\ell L \delta u_\ell dr. \quad (7)$$

The first term on the RHS of Eq. (7) vanishes because $L u_\ell = 0$ and the second term can be further simplified by using Eqs. (3) and (4). The result is

$$\delta L = -\frac{k}{2} W \delta \lambda + \int_0^\infty \delta u_\ell(r) L \delta u_\ell(r) dr, \quad (8)$$

where W is the Wronskian defined by

$$\begin{aligned} W &= F_\ell(x) \frac{d}{dx} G_\ell(x) - G_\ell(x) \frac{d}{dx} F_\ell(x) \\ &= \text{constant}. \end{aligned} \quad (9)$$

Equation (8) is known as the Kato identity, and expresses the exact value of λ in terms of the approximate value of the functional L and a term which is second order in the error in the wave function. The Kato identity thus provides a stationary principle for approximating λ :

$$\lambda^s = \lambda^t + \frac{2}{kW} \int_0^\infty u_\ell^t L u_\ell^t dr. \quad (10)$$

The stationary principle can be solved explicitly for a wave function that contains only linear trial coefficients. If we choose a trial wave function of the form

$$u_\ell^t = f_\ell(r) + \lambda^t g_\ell(r) + \sum_{i=1}^n c_i \varphi_i, \quad (11)$$

with

$$\begin{aligned} f_\ell(r) &\underset{r \rightarrow \infty}{\sim} F_\ell(kr), \\ g_\ell(r) &\underset{r \rightarrow \infty}{\sim} G_\ell(kr), \end{aligned} \quad (12)$$

and with $\{\varphi_i\}$ a set of square-integrable functions, then the coefficients λ^t and c_i are determined by making Eq. (10) stationary:

$$\frac{\partial \lambda^s}{\partial c_i} = \frac{\partial \lambda^s}{\partial \lambda^t} = 0. \quad (13)$$

Substituting Eq. (11) into Eq. (10) and taking the derivative with respect to c_i gives

$$\int_0^\infty \varphi_i L u_\ell^i dr = 0, \quad i = 1, \dots, n, \quad (14)$$

while differentiation with respect to λ^t gives, after some rearrangement,

$$\int_0^\infty g_\ell L u_\ell^i dr = 0, \quad (15)$$

where we have again used the relation

$$\int_0^\infty f_\ell L g_\ell dr = -\frac{1}{2} kW + \int_0^\infty g_\ell L f_\ell. \quad (16)$$

If we relabel the basis functions $g_\ell(r)$ and $\varphi_i(r)$ into a single set $\{\varphi_i\}$, $i = 0, \dots, n$ with $\varphi_0 = g_\ell$, and denote the linear parameters $(\lambda^t, c_1, \dots, c_n)$ by the vector c , then Eqs. (14) and (15) can be expressed in the compact form

$$c = -M^{-1}s \quad (17)$$

where M is a matrix with elements

$$M_{ij} = \int_0^\infty \varphi_i L \varphi_j dr, \quad i, j = 0, \dots, n, \quad (18)$$

and s is a vector with elements

$$s_i = \int_0^\infty \varphi_i L f_\ell dr, \quad i = 0, \dots, n. \quad (19)$$

The desired expression for the stationary value of λ^s is obtained by substituting Eq. (17) into Eq. (10) to obtain:

$$\lambda^s = \frac{2}{kW} \left[\int_0^\infty f_\ell L f_\ell dr - s M^{-1} s \right]. \quad (20)$$

The exact form of the free functions F_ℓ and G_ℓ has yet to be specified. We can take F_ℓ (and f_ℓ) to be the regular Riccati-Bessel function²⁵ $j_\ell(kr)/\sqrt{k}$. The traditional choice for G_ℓ is the irregular Riccati-Neuman function $n_\ell(kr)/\sqrt{k}$. The function g_ℓ , which must be regular at $r = 0$, is usually obtained by multiplying G_ℓ by a suitable cut-off function that

approaches unity for large r . With this choice, $W = 1/k$, λ is simply the tangent of the phase shift, $\tan \delta_\ell$, and Eq. (20) reduces to the familiar Kohn variational expression for $\tan \delta_\ell^*$. Note that M is a real symmetric matrix in this case, and has zero determinant at the real values of E corresponding to the eigenvalues of H in the basis of φ_i plus g_ℓ . At these energies, Eq. (20) is singular; this is the origin of the so-called Kohn anomalies.¹⁶

If G_ℓ is chosen to be the outgoing Hankel function $h_\ell^+(kr)/\sqrt{k}$, defined as

$$h_\ell^+(kr)/\sqrt{k} = i[j_\ell(kr) + in_\ell(kr)]/\sqrt{k}, \quad (21)$$

then $W = -1/k$ and Eq. (20) becomes an expression for the T -matrix, $\lambda = T_\ell = e^{i\delta_\ell} \sin \delta_\ell$:

$$T_\ell^s = -2 \left[\int_0^\infty f_\ell L f_\ell dr - s M^{-1} s \right]. \quad (22)$$

M is now a complex symmetric matrix, and its inverse is generally nonsingular at real energies.¹⁹ We thus call this form of the variational equations the complex Kohn method. While M^{-1} can, in principle, be singular at a real energy, such an occurrence is improbable and is not a problem in practical calculations.

2.2. Continuum Basis Functions

As we have stated, the traditional choice for continuum basis functions in Kohn-type variational calculations is to use spherical Bessel or, for ionic targets, Coulomb-Bessel functions, regularized at $r = 0$ by a simple exponential cut-off. This choice was historically motivated by the desire to develop analytic procedures for evaluating the required one- and two-electron matrix elements.²⁶ Although this approach was practical for atomic applications, it did not represent a viable approach to electron-molecule scattering problems, a fact which undoubtedly explains why progress in applying Kohn-type methods in the latter area had to await further theoretical developments. We will see below that the continuum matrix elements required are of a limited class and can all be efficiently evaluated by adaptive three-dimensional quadrature schemes, even for non-linear polyatomic targets. This allows for considerable flexibility in the choice of continuum basis functions, since the method no longer relies on any particular analytic technique.

In early calculations with the complex Kohn method, we noticed some sensitivity in the results to the way in which the outgoing wave continuum functions were cut off near the origin. The problem was more severe near elastic or inelastic thresholds, particularly for ionic targets. This difficulty prompted us to seek a more physically motivated choice for regularizing the outgoing wave continuum basis functions needed in the complex Kohn method.²⁷ The choice we made was inspired by the recent work of Sun et al.²⁸ on the Kohn and generalized Newton variational principles.

A more physical choice for the outgoing continuum functions is suggested by considering the behavior of the exact wave function u_ℓ^+ , for single-channel scattering by a potential V . This function satisfies the Lippmann-Schwinger equation

$$u_\ell^+ = F_\ell + G_\ell^+ V u_\ell^+, \quad (23)$$

where G_ℓ^+ is the radial partial-wave free-particle Green's function, which is defined here as²⁹

$$G_\ell^+(r, r') = \begin{cases} -2/kj_\ell(kr)h_\ell^+(kr'), & r \leq r', \\ -2/kj_\ell(kr')h_\ell^+(kr), & r > r'. \end{cases} \quad (24)$$

For the purpose of defining a new outgoing wave function in a complex Kohn trial wave function, the scattered wave part of u_ℓ^+ , which is defined as $G_\ell^+ V u_\ell^+$, can be replaced by its Born approximation:

$$g_\ell(r) = AG_\ell^+ VF_\ell. \quad (25)$$

The constant A is introduced in order to normalize $g_\ell(r)$, as in Eq. (21), and is thus given by

$$A = \left[2 \int_0^\infty F_\ell V F_\ell dr \right]^{-1}. \quad (26)$$

All that is formally required of the "test potential" V is that it diverge less strongly than $1/r^2$ at the origin, and go to zero faster than $1/r$ at infinity. It is otherwise arbitrary. One might consider choosing V to incorporate some property of the full interaction potential, but we have not found this to be a necessary requirement. Choosing V to be a simple exponential function gives significantly better convergence properties than the usual cut-off

basis function technique. It is interesting to note that the functions defined in Eqs. (25) and (26) have the property that

$$\text{Im}(g_\ell) = F_\ell. \quad (27)$$

The function g_ℓ is easily calculated by noting that it satisfies the inhomogeneous differential equation

$$\left(\frac{d^2}{dr^2} - \frac{\ell(\ell+1)}{r^2} + 1 \right) g_\ell(r) = 2AVF_\ell(r). \quad (28)$$

It is a simple matter to construct the function required in Eq. (25) as a linear combination of a solution to Eq. (28) obtained by numerical integration and a solution of the corresponding homogeneous equation. This technique has the added advantage of not requiring the irregular function G_ℓ on the integration mesh.²⁷

2.3. Trial Wave Function for Multichannel Scattering

We will consider the electron-molecule scattering problem in body-frame coordinates within the framework of the fixed-nuclei approximation. We use a trial wave function of the form³⁰

$$\Psi_{\Gamma_0} = \sum_{\Gamma} A(\chi_{\Gamma} F_{\Gamma\Gamma_0}) + \sum_{\mu} d_{\mu}^{\Gamma_0} \Theta_{\mu}. \quad (29)$$

The first sum runs over a set of energetically open N -electron target states, χ_{Γ} . $F_{\Gamma\Gamma_0}$ is a one-electron function that describes the scattered electron; the index Γ_0 labels a particular degenerate solution corresponding to the initial state of the target. The operator A antisymmetrizes the orbital functions $F_{\Gamma\Gamma_0}$ into the functions χ_{Γ} . Note that we are using the symbol Γ to label all the quantum numbers needed to represent a physical state of the composite system, that is, the internal state of the target and the angular momentum of the scattered electron. It is assumed that $F_{\Gamma\Gamma_0}$ is, by construction, orthogonal to all the orbital functions used to construct χ_{Γ} . The functions Θ_{μ} are a set of configuration state functions (CSF's) constructed from square-integrable (Cartesian Gaussian) functions. They are used to represent polarization and correlation effects not included in the first summation. The second sum will also contain any terms needed to

relax any constraint on the total wave function implied by the orthogonality requirement imposed on $F_{\Gamma\Gamma_0}$.

In the complex Kohn method, the functions $F_{\Gamma\Gamma_0}$ are further expanded as

$$F_{\Gamma\Gamma_0} = \sum_i c_i^{\Gamma\Gamma_0} \varphi_i + \sum_{\ell m} [f_\ell^\Gamma(k_\Gamma r) \delta_{\ell\ell_0} \delta_{mm_0} \delta_{\Gamma\Gamma_0} + T_{\ell\ell_0 mm_0}^{\Gamma\Gamma_0} g_\ell^\Gamma(k_\Gamma r)] Y_{\ell m}(\hat{r})/r, \quad (30)$$

where the φ_i are a set of square-integrable functions, $Y_{\ell m}$ is a normalized spherical harmonic, and the functions f_ℓ^Γ and g_ℓ^Γ are the regular and outgoing-wave continuum functions discussed in the previous section. The channel momenta k_Γ are determined by energy conservation,

$$k_\Gamma^2/2 = E - E_\Gamma, \quad (31)$$

where E is the total energy of the composite system and E_Γ is the energy of the target molecule corresponding to state χ_Γ . The coefficients $T_{\ell\ell_0 mm_0}^{\Gamma\Gamma_0}$ are elements of the T -matrix and are the fundamental dynamical quantities from which differential and integral cross-sections are constructed. In order to simplify the notation in what follows, we will adopt the convention of using $f_{\ell m}^\Gamma$ (or $g_{\ell m}^\Gamma$) to denote the product of a radial function f_ℓ^Γ (or g_ℓ^Γ) and $Y_{\ell m}/r$.

The expansion given by Eq. (29) is quite general, and is common to many close-coupling formulations. Methods which use a wave function expansion of this type are generally referred to as close-coupling plus correlation (CCPC) methods. The variational expansion of the orbital functions $F_{\Gamma\Gamma_0}$ given in Eq. (30) is the generalization of Eq. (11) to the multichannel case. The target functions χ_Γ may be single- or multiconfiguration descriptions of the bound states of the molecule. For practical reasons, the orbital space used to generate these states should be kept manageably small; average natural orbital techniques are ideal in this connection, and will be further discussed below.

Because the first sum in Eq. (29) is restricted to those target states which are energetically open, it cannot be made complete even in principle; closed channels are required for completeness. However, since the closed-channel contributions to the wave function fall off exponentially as any electron coordinate tends to infinity, they can be incorporated into the wave function through appropriate contributions to the second sum in Eq. (29).

The $(N+1)$ -electron CSF's which comprise this part of the wave function can generally be classified into three distinct types:

- (i) Penetration terms: These are simply those terms needed to relax any constraint implied by requiring $F_{\Gamma\Gamma_0}$ to be orthogonal to the orbitals used to build the χ_Γ .³⁰
- (ii) CI relaxation terms: If multiconfiguration target states are used, then the χ_Γ will be constructed as fixed linear combinations of CSF's. There is an orthogonal complement of target states, presumed to be energetically closed, that uses the same CSF's in different linear combinations. The CI relaxation terms are built as the direct product of these states and a square-integrable orbital.³¹
- (iii) Polarization terms: Additional closed channels can also be incorporated in the trial wave function by adding terms which are the direct product of a bound orbital and a disjoint set of target configurations. Such terms are very important in describing the polarization effects that can dominate the scattering cross-sections at low energy.³² It is important to realize that constraints apply to the class of $(N+1)$ -electron configuration state functions, Θ_μ , that account for polarization and correlation in the scattering wave function. In particular, these terms must not introduce N -electron correlation terms which were not included in the determination of the $(N$ -electron) target wave functions. CSF's with this unphysical character are referred to as "recorrelation terms" and can give rise to a scattering potential which is too attractive.

In principle, the total wave function can be described to any desired level of accuracy with a trial wave function of the form just outlined. In practice, since the open-channel expansion is usually truncated rather severely and the target states themselves are approximate, it is very important to balance correlation effects in the N - and $(N+1)$ -electron systems in the process of deciding what types of terms are reasonable to include in the trial wave function.

2.4. P- and Q-Space Partitioning

It is convenient to partition the total wave function into two parts, $P\Psi_{\Gamma_0}$ and $Q\Psi_{\Gamma_0}$, corresponding to the two sums defined in Eq. (29). Since $Q\Psi_{\Gamma_0}$ is square-integrable, it is not explicitly needed for the determination of

scattering parameters. As we previously stated, the channel orbitals $F_{\Gamma\Gamma_0}$ in the Kohn method are expanded as linear combinations of bound and continuum functions. All these functions can be mutually orthogonalized without changing the resulting T -matrix, a property known as transfer invariance.¹⁵ We have also followed the common practice of requiring the channel orbitals to be orthogonal to all the bound-state orbitals which are used to form the target wave functions, and have commented that these additional constraints, if necessary, can be relaxed by including appropriate penetration terms in $Q\Psi_{\Gamma_0}$.^{33,34}

In calculations which include the effect of closed channels, the set of Q -space configurations can become quite large. For this reason, and because of the fact that the configuration state functions $\{\Theta_\mu\}$ are built solely from square-integrable orbitals, it is desirable to use bound-state molecular structure methods to treat the Q -space portion of the problem and to divorce this part of the calculation from the rest of the variational calculation. This can be done by using the formalism of Feshbach partitioning.³⁵

Defining M as $(H - E)$, we can derive in the usual way a modified Hamiltonian that determines $P\Psi$:

$$\begin{aligned} H_{\text{eff}} &= H_{PP} - M_{PQ}M_{QQ}^{-1}M_{QP} \\ &= H_{PP} - V_{\text{opt}}, \end{aligned} \quad (32)$$

where M_{QQ}^{-1} is the inverse of the Hamiltonian matrix spanned by the functions $\{\Theta_\mu\}$. This allows us to drop the variational coefficients $d_\mu^{\Gamma_0}$ in Eq. (29) from further consideration. We can now proceed to use the effective Hamiltonian defined in Eq. (32) to define a functional, just as we did in the single-channel case, for the purpose of getting a stationary approximation to the T -matrix. The multichannel T -matrix can again be characterized as the stationary value of the Kohn functional

$$T_s^{\Gamma\Gamma'} = T_t^{\Gamma\Gamma'} - 2 \int \Psi_\Gamma(H_{\text{eff}} - E)\Psi_{\Gamma'} dr_1 \dots dr_{N+1}. \quad (33)$$

By following the same procedures outlined in Sec. 2.1, we obtain the generalization of Eq. (22):

$$T_s = -2(M_{00} - M_{q0}^t M_{qq}^{-1} M_{q0}), \quad (34)$$

where we have used a condensed matrix notation, in which open-channel indices are suppressed. The index 0 denotes the subspace spanned by the functions $\{\chi_\Gamma f_\ell^\Gamma Y_{\ell m}/r\}$ and the index q refers to the subspace spanned by $\{\chi_\Gamma g_\ell^\Gamma Y_{\ell m}/r\}$ and $\{\chi_\Gamma \varphi_i\}$. M refers to the operator $(H_{\text{eff}} - E)$. For example, the elements of M_{00} are defined as

$$(M_{00})_{\ell m \ell' m'}^{\Gamma\Gamma'} = \int A(\chi_\Gamma f_\ell^\Gamma)(H_{\text{eff}} - E)A(\chi_{\Gamma'} f_{\ell' m'}^{\Gamma'}) dr_1 \dots dr_{N+1}, \quad (35)$$

and M_{q0} and M_{qq} are defined similarly.

We have been a bit careless up to this point by not specifying how one is to treat complex conjugation in the definition of matrix elements. To remove any ambiguity, the trial wave function and the basis functions $g_{\ell m}^\Gamma \equiv g_\ell^\Gamma Y_{\ell m}$ should be given a "+" or "-" label to denote outgoing- or incoming-wave boundary conditions. With reference to the Kohn functional defined in Eq. (33) then, $\Psi_{\Gamma'}$ should be replaced by $\Psi_{\Gamma'}^+$ and Ψ_Γ should be replaced by Ψ_Γ^{-*} . By noting that $g_\ell^{\Gamma-*} = g_\ell^{\Gamma+}$, we conclude that all conjugate vectors φ^\dagger that appear in matrix elements of the form $\int \varphi^\dagger M \zeta$ must be evaluated by complex conjugating angular basis functions only, and not radial functions. Thus M_{qq} , for example, will be a complex symmetric matrix.

The variational calculation requires the construction of various types of matrix elements of H_{eff} and the solution of a complex set of linear equations. The matrix elements can be classified as either free-free, bound-free or bound-bound, depending upon whether two, one or zero continuum orbitals appear in the expression. The bound-bound terms, which generally constitute the largest class of matrix elements, can be evaluated using bound-state structure methodology. The bound-free and free-free terms must be handled numerically. Since the methods employed in evaluating these various Hamiltonian matrix elements are quite different, it is critical that we have some way of guaranteeing a consistent set of definitions for defining and ordering CSF's and establishing phase conventions. We will discuss the bound-bound problem first.

The effective Hamiltonian defined in Eq. (32) is an $(N + 1)$ -electron operator in a product space of functions defined by the first term in Eq. (29) and labeled by open target channels. Operationally, we must reduce this many-electron operator to a matrix of one-electron operators defined over the functions used to expand $F_{\Gamma\Gamma_0}$ by integrating out the N -coordinates of the target. The electronic structure problem, then, consists of two distinct

tasks. We have first an N -electron problem in which a set of target wave functions are determined by a CI expansion in which a set of molecular orbitals, which we call target orbitals, are used. We then have an $(N+1)$ -electron problem in which a complementary set of "scattering" orbitals, distinct from and orthogonal to the target orbitals, are combined in direct products with the target wave functions — these are the P -space configurations. The $(N+1)$ -electron problem also involves Q -space configurations which are not in general labeled by target channels. The Q -space configurations of the "penetration" type are built entirely from target orbitals, while the relaxation and polarization configurations can involve both target and scattering orbitals.

The procedures we employ for carrying out the contraction of the Hamiltonian with respect to the P -space target wave functions warrants explanation in some detail.³¹ We reiterate that it is essential to insure consistency between the N -electron and $(N+1)$ -electron problems with respect to phase conventions, ordering of configurations, etc. This may be difficult with molecular structure codes which make provision for automatic generation of configurations, since these conventions may not be transparent. To avoid any possible ambiguity, we determine the target CI coefficients from a pseudo- $(N+1)$ -electron CI calculation, which is performed in the following manner. Let $\{\Phi_i\}$, $i = 1, \dots, n$ denote the N -electron configurations used to expand the target eigenstates. We first set up an $n \times n$ Hamiltonian in the $(N+1)$ -electron space, where each configuration is a direct product of a Φ_i and a single square-integrable function, φ_s , which represents the scattering electron. However, before carrying out this CI calculation, all one- and two-electron integrals involving φ_s are set to zero. Because there is no interaction between φ_s and the remaining N electrons, the diagonalization of this Hamiltonian will produce the desired N -electron target states.

Let $\{c_i^r\}$, $i = 1, \dots, n$ denote the CI expansion coefficients of these target eigenstates. P -space is constructed from the m ($m \leq n$) eigenvectors of this Hamiltonian associated with energetically open channels. Moreover, this set of target vectors can serve as prototypes for building a new set of vectors for use in the full $(N+1)$ -electron problem, in which a Hamiltonian is built from repeated products of the target configurations $\{\Phi_i\}$ and all the scattering orbitals in succession, $\{\varphi_j\}$, $j = 1, \dots, p$. Penetration and polarization configurations, which are denoted by Θ_q , are appended to the end

of this list. The full Hamiltonian before transformation has the structure:

$$H = \begin{bmatrix} H_{11}^{11} \cdots H_{1n}^{11} & H_{11}^{12} \cdots H_{1n}^{1p} & H_{1Q}^1 \\ \vdots & \vdots & \vdots \\ H_{n1}^{11} & H_{nn}^{11} & H_{n1}^{12} & H_{nn}^{1p} & H_{nQ}^1 \\ H_{11}^{21} & H_{1n}^{21} & H_{11}^{22} & H_{1n}^{2p} & H_{1Q}^2 \\ \vdots & \vdots & \vdots & \vdots & \vdots \\ H_{n1}^{p1} & H_{nn}^{p1} & H_{n1}^{p2} & H_{nn}^{pp} & H_{nQ}^p \\ H_{1Q}^{1\dagger} \cdots H_{nQ}^{1\dagger} & H_{1Q}^{2\dagger} \cdots H_{nQ}^{p\dagger} & H_{QQ} & & \end{bmatrix}, \quad (36)$$

where

$$H_{ij}^{kl} = \langle \Phi_i \varphi_k | H | \Phi_j \varphi_l \rangle, \quad (37)$$

and

$$H_{iq}^j = \langle \Phi_i \varphi_j | H | \Theta_q \rangle. \quad (38)$$

The vectors used to transform the Hamiltonian matrix can be arranged into a rectangular matrix U of dimension $n \times p+Q$ by $m \times p+Q$,

$$U = \begin{bmatrix} c_1^1 c_1^2 \cdots c_1^m & & & & \\ \vdots \vdots \vdots & 0 & 0 & & \\ c_n^1 c_n^2 \cdots c_n^m & & & & \\ & & & & \\ & & & & \\ & & & & \\ c_1^1 c_1^2 \cdots c_1^m & & & & \\ 0 & \vdots & \vdots & \vdots & 0 \\ & & & & \\ c_n^1 c_n^2 \cdots c_n^m & & & & \\ 0 & 0 & 0 & & 1 \end{bmatrix}, \quad (39)$$

where 1 denotes a unit matrix of the full dimension of Q -space. The bound-bound portion of H_{eff} is obtained by partitioning $U^\dagger H U$. The prototyping scheme we have outlined removes any possible inconsistencies between the

N - and $(N+1)$ -electron problems and preserves the phase conventions used in the original determination of the target states. The procedure can also be modified if we wish to take specific account of the symmetry of the various open-channel target states. In that case, we would first group the target CSF's into different symmetry classes and then use a different prototype orbital, φ_s^A , for each class in order to couple up to a specific total symmetry, A .

The Q -space configurations, from which the optical potential is built, consist of the penetration and polarization terms explicitly included as Θ_q , and the CI relaxation terms to which we now turn our attention. Recall that the P -space vectors were constructed as direct products of scattering orbitals and a fixed number, m , of eigenstates of an $n \times n$ Hamiltonian matrix. The complement of P -space consists of the direct product of the scattering orbitals and the remaining $(n - m)$ target eigenstates, which are presumed to be energetically closed. The algorithm that is used to include the CI relaxation terms in Q -space does *not* require the determination of all of the eigenvectors of the target Hamiltonian. Rather, we employ projection operators to account for these terms and can thereby avoid the explicit construction of H_{QQ} . In building the optical potential defined by Eq. (32), H_{QQ} is used to solve a set of linear equations,

$$(E - H_{QQ})X_{QP} = H_{QP}, \quad (40)$$

and

$$V_{PP}^{\text{opt}} = H_{PQ}X_{QP} = H_{PQ}(E - H_{QQ})^{-1}H_{QP}. \quad (41)$$

This equation is solved in the configuration state function basis rather than in the basis of CI eigenfunctions.³⁶ Thus

$$\begin{aligned} H_{QQ} &= \begin{bmatrix} 1 - |C_p\rangle\langle C_p| & 0 \\ 0 & 1 \end{bmatrix} \begin{bmatrix} H_{ij}^{kl} & H_{iq}^k \\ H_{iq}^{kl} & H_{qq} \end{bmatrix} \begin{bmatrix} 1 - |C_p\rangle\langle C_p| & 0 \\ 0 & 1 \end{bmatrix} \\ &\equiv \rho_Q \begin{bmatrix} H_{ij}^{kl} & H_{iq}^k \\ H_{iq}^{kl} & H_{qq} \end{bmatrix} \rho_Q \\ &\equiv \rho_Q H^{\text{CSF}} \rho_Q, \end{aligned} \quad (42)$$

where

$$C_p = \begin{bmatrix} c_1^1 & \dots & c_1^m \\ \vdots & \ddots & \vdots \\ c_n^1 & \dots & c_n^m \\ 0 & & 0 \\ & c_1^1 & c_1^m \\ & \vdots & \vdots \\ & c_n^1 & c_n^m \end{bmatrix} \quad (43)$$

The linear equations, Eq. (40), are solved iteratively by successively multiplying $(E - H_{QQ})$ by a set of trial vectors, $(X^i, i = 1, \dots, r)$ and solving a small set of linear equations in the trial space until convergence is achieved. This type of algorithm has been discussed in a number of papers and a detailed description will not be given here.³⁷ We only note that neither the projection operator, ρ_Q , nor the Q -space Hamiltonian, H_{QQ}^{CSF} , need be explicitly constructed.³⁶ The multiplication of the trial vector, X^i , by $(E - H_{QQ})$ is conducted in a series of vectorizable steps

$$\begin{aligned} \text{a. } \rho_Q X^i &= (1 - |C_p\rangle\langle C_p|)X^i \\ &= |X^i\rangle - |C_p\rangle\langle C_p|X^i \\ &\equiv X_P^i, \\ \text{b. } (E - H_{QQ}^{\text{CSF}})X_P^i &= R_Q^i, \\ \text{c. } \rho_Q R_Q^i &= |R_Q^i\rangle - |C_p\rangle\langle C_p|R_Q^i\rangle. \end{aligned} \quad (44)$$

A direct-CI procedure can be used to perform the multiplication of $(E - H_{QQ}^{\text{CSF}})$ times the projected trial function. This is a standard procedure in most modern electronic structure packages, and allows us to employ large Hamiltonian matrices in the scattering calculations.³⁸ In cases where the Q -space is very large, the procedure just outlined for obtaining V_{opt} will be far more efficient than explicitly inverting $(E - H_{QQ})$.

2.5. Separable Expansions

While the techniques of bound-state structure theory can be used to evaluate bound-bound matrix elements, the matrix elements involving continuum basis functions are more problematic and the principal difficulty

of any molecular scattering calculation is their evaluation. There are two critical steps in making this problem tractable for polyatomics. The first step uses separable approximations to eliminate an entire class of continuum exchange and optical potential matrix elements.³⁹ The second step is the development of an efficient numerical technique for evaluating the remaining continuum matrix elements. We explain the first step here.

We must first explain what is meant by the separable representation of an operator. A separable representation of an operator can be achieved by projection onto a finite basis⁴⁰:

$$H \approx \sum_{\alpha\beta} |\varphi_\alpha\rangle H_{\alpha\beta} \langle\varphi_\beta|. \quad (45)$$

With reference to the effective Hamiltonian defined in Eq. (32), this type of representation is invoked for the exchange components of H_{PP} , as well as V_{opt} . The basis we use for this separable representation is the set of target orbitals, along with the square-integrable functions used to expand the channel orbitals $F_{\Gamma\Gamma_0}$. To see the usefulness of such representations, consider the expansion of the channel functions $F_{\Gamma\Gamma_0}$ given in Eq. (30). If we were to add any multiple of the square-integrable basis functions φ_i to the continuum functions f_ℓ^Γ and g_ℓ^Γ , the asymptotic form of $F_{\Gamma\Gamma_0}$ would of course remain unchanged. The process simply transfers a square-integrable term from the first sum to the second. The Kohn variational equations have the property of *transfer invariance*, which means that the T -matrix elements are invariant to such a transformation.¹⁵ We can therefore require the continuum basis functions to be orthogonal to the functions φ_i . Now we also require the continuum functions to be orthogonal to the orbitals used to construct the target wave functions. The T -matrix elements, however, are not in general invariant to this latter transformation of the expansion basis, so appropriate Q -space terms must be included in the optical potential to relax these "target orthogonality" constraints.^{30,33,34}

Now consider a continuum matrix element, for example, a free-free matrix element of the type defined in Eq. (35). It is useful to separate this integral into a direct component,

$$\begin{aligned} \text{Direct } (M_{00}^{PP})_{\ell m \ell' m'}^{\Gamma \Gamma'} &\equiv \int \chi_\Gamma(r_1 \dots r_N) f_{\ell m}^\Gamma(r_{N+1}) (H_{PP} - E) \\ &\times \chi_{\Gamma'}(r_1 \dots r_{N+1}) f_{\ell' m'}^{\Gamma'}(r_{N+1}) dr_1 \dots dr_{N+1}, \end{aligned} \quad (46)$$

and an exchange component arising from the interchange of "bound" and "free" electron coordinates. We have previously shown that the short-range character of the exchange operators allows for their expansion in a rapidly convergent series of separable terms.^{39,40} The separable expansion of exchange terms leads to a great simplification in the present context. Indeed, if the exchange operators are projected onto a finite set of $(N+1)$ -electron configurations, Λ_m , which are made up from the entire set of target plus scattering square-integrable basis orbitals, then all free-free and bound-free exchange integrals will simply vanish. This is a consequence of the strict orthogonality condition we have imposed on the continuum functions, i.e.,

$$\begin{aligned} \text{Exchange } (M_{00}^{PP})_{\ell m \ell' m'}^{\Gamma \Gamma'} &\approx \sum_{m,n} \langle A(\chi_\Gamma f_{\ell m}^\Gamma) | \Lambda_m \rangle \\ &\times \langle \Lambda_m | (H_{pp} - E) | \Lambda_n \rangle \langle \Lambda_n | A(\chi_{\Gamma'} f_{\ell' m'}^{\Gamma'}) \rangle \\ &= 0, \end{aligned} \quad (47)$$

since $\langle \Lambda_n | A(\chi_{\Gamma'} f_{\ell' m'}^{\Gamma'}) \rangle = 0$. The presumption is that, since the exchange interactions are relatively short-ranged, the square-integrable basis can be made large enough to make this a good approximation. Similarly, matrix elements involving continuum functions and $(N+1)$ -electron CSF's are also expanded in a square-integrable basis:

$$(A(\chi_\Gamma f_{\ell m}^N) | (H - E) | \Theta) \approx \sum_m \langle A(\chi_\Gamma f_{\ell m}^\Gamma) | \Lambda_m \rangle \langle \Lambda_m | (H - E) | \Theta \rangle = 0. \quad (48)$$

The consequence of these approximations is that no continuum matrix elements involving either exchange or optical interactions need be constructed, and the entire effect of these interactions is carried in the bound-bound portions of the Hamiltonian. Whether or not this is a good approximation depends upon how many functions we include in the underlying L^2 basis and how close it comes to being complete for the purpose of representing the operators in question. In this context, one must bear in mind that the orbitals used in the determination of target wave functions must necessarily be excluded from the set of L^2 functions used to expand the channel scattering functions. There is no formal difficulty here, since these target orbitals, as we have stated, appear in appropriate $(N+1)$ -electron "penetration" terms in Q -space. However, because the optical potential is only

represented in separable form, the transference of terms from P -space to Q -space does involve an approximation. For this reason, we try to keep the target orbital space as compact as possible.

2.6. Adaptive Quadrature

There is no justification for using separable expansions to treat long-range direct interactions, so we handle these terms numerically. The direct integrals may be expressed in terms of one-particle transition potentials. For example, we can write

$$\langle A(\chi_i f) | (H - E) | A(\chi_j g) \rangle_{\text{direct}} = \delta_{ij} \langle f | -1/2\nabla^2 + E_i - E + V_{\text{nuc}} | g \rangle + \langle f | V_{ij} | g \rangle, \quad (49)$$

where

$$V_{ij}(r) = \sum_{q=1,N} \int \chi_i(\hat{r}_1 \dots \hat{r}_N) \frac{1}{|r - r_q|} \chi_j(\hat{r}_1 \dots \hat{r}_N) dr_1 \dots dr_N. \quad (50)$$

The integrals in Eq. (49) may thus be reduced to three-dimensional quadrature.

The quadrature scheme we will describe⁴¹ is applied only to the evaluation of the bound-free and free-free matrix elements of direct potential operators and of the kinetic energy. This procedure provides a set of points and weights in the space $r = (x, y, z)$. The prerequisite for the quadrature is that we be able to construct the integrand at points in three-space. For example, for a bound-free potential matrix element, $\langle \varphi_k | V_{\text{nuc}} + V_{\Gamma\Gamma'} | g_{\ell'm'}^{\Gamma'} \rangle$, we need Gaussian basis functions which contribute to φ_k , a continuum function defined in Eq. (25), and a spherical harmonic evaluated at the points in r -space, as well as the potential $V_{\Gamma\Gamma'}(r)$. The Gaussian functions and nuclear attraction potential, V_{nuc} , are of course given by simple formulas, the spherical harmonic functions can be evaluated by straightforward recursion schemes and the continuum functions by the schemes outlined in Sec. 2.2. The direct potential from Eq. (50) can be written in terms of the one-electron density matrix (or transition density matrix if $\Gamma \neq \Gamma'$), $\rho^{\Gamma\Gamma'}$:

$$V_{\Gamma\Gamma'}(r) = \sum_{kk'} \rho_{kk'}^{\Gamma\Gamma'} \int \frac{\varphi_k(r)\varphi_{k'}(r')d^3r'}{|r - r'|}. \quad (51)$$

The density matrices are constructed with the target state vectors obtained from the pseudo- $(N+1)$ -electron CI previously described to assure consistency between the numerically and analytically obtained matrix elements. The bound functions, φ_k , appearing in Eq. (51) are simply sums of Gaussians, so the integrals appearing in this equation are identical to nuclear attraction integrals with a nucleus at the position r . These integrals are one-electron integrals which appear in any quantum chemistry computer code. An efficient algorithm can be constructed which computes these for the r points in the quadrature grid, and which can easily make use of vectorization on vector architecture supercomputers. We can thus construct the factors of the integrands of the bound-free and free-free integrals which we require at points in a three-dimensional quadrature grid.⁴² We now turn our attention to the construction of the points and weights of the grid.

We will choose a single grid with which to quadrature all integrals involving free functions. The integrands of many of those integrals involve nuclear singularities or bound functions which are strongly peaked at the nuclei, so we must adapt our quadrature accordingly. It is near the integrable singularities of the nuclear potentials that we must use the greatest care to avoid quadrature errors. Asymptotically, however, the integrands of many of our integrals, the free-free integrals, become separable in spherical coordinates. For large r the potential ultimately is proportional to a single spherical harmonic (the largest term in a multipole expansion) and the free functions are products of Bessel functions and spherical harmonics. So our grid should make a smooth transition from local spherical symmetry around each nuclear singularity to global spherical symmetry around the center of charge of the molecule.

To construct such a quadrature, consider the general three-dimensional integral

$$I = \int F(r) d^3r, \quad (52)$$

and define the change of variable:

$$r(q) = q - \sum_{\text{nuc}} (q - R_{\text{nuc}}) S_{\text{nuc}}(q), \quad (53)$$

where $S_{\text{nuc}}(q)$ is a strength function depending on the distance of a point from the nuclear position R_{nuc} . The function $S_{\text{nuc}}(q)$ may be chosen in any number of ways, but it must have the property that it go to zero as

$q \rightarrow \infty$. This property is necessary so that the transformation in Eq. (53) will reduce to the identity, and r will be the same as q at large distances from the molecule. A flexible and effective form for our purpose is

$$S_{\text{nuc}}(q) = P(|q - R_{\text{nuc}}|)^2 / \sum_{\text{nuc}'} P(|q - R_{\text{nuc}'}|), \quad (54)$$

where the sum is over all nuclei in the molecule and

$$P(\zeta) = e^{-\mu\zeta^2}. \quad (55)$$

The effect of this transformation is to draw points in q -space toward R_{nuc} if they lie roughly within a radius of $1/\mu$ of R_{nuc} and to leave them unaffected otherwise. With this change of variable, the integral we wish to evaluate becomes

$$I = \int F(r(q)) |\partial r / \partial q| d^3 q. \quad (56)$$

This equation is equivalent to Eq. (52) only if the transformation from q to r is one to one. The particular form we have chosen for $S_{\text{nuc}}(q)$ makes this constraint easy to accomplish. We have found that for values of μ between 5 and 20 the transformation is well-behaved for internuclear distances of two bohr radii and up.

The first step in developing an optimum and efficient grid for a particular molecule is to choose a separable (q, θ_q, φ_q) grid consisting of shells of points chosen from standard one-dimensional quadratures. In our calculations, we have used Gauss-Legendre quadratures on subintervals of q and $\cos(\theta_q)$ and Simpson's rule for φ_q . Although this grid is separable, it can be adapted to the molecular framework by choosing the (q, θ_q, φ_q) grid to have a denser spacing of points in those subshells which contain the nuclei, as shown in the two-dimensional projection of such a grid in Fig. 1(a). Then, upon evaluating the Jacobian of the transformation at each point and defining

$$w_p = w_{q_p} w_{\theta_{q_p}} w_{\varphi_{q_p}}, \quad (57)$$

we obtain

$$I = \sum_p F(r(q_p)) |\partial r / \partial q_p| w_p, \quad (58)$$

where the sum is over points in the q grid.

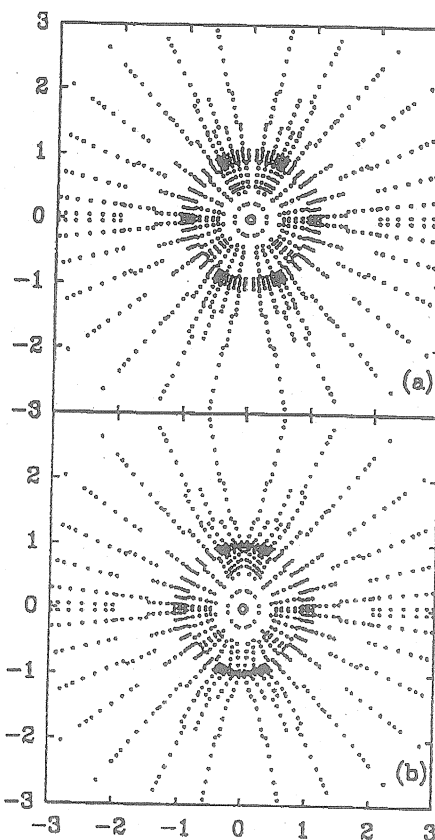


Fig. 1. (a) Sample untransformed (separable) grid for a case with two atoms, located vertically $\pm 1 a_0$ from figure center. (b) Same grid after transformation, showing condensation of points near the atoms.

Equation (58) defines a nonseparable, adaptive three-dimensional quadrature with effective weight $|\partial r / \partial q_p| w_p$ at each point grid. Figure 1(b) shows the transformed grid $r(q)$ for a sample grid. One can, of course, use molecular symmetry to reduce the number of numerical grid points that may be needed for a particular problem. For example, in the two-dimensional example shown in Fig. 1(b), only one quarter of the points shown are symmetry-unique.

2.7. Cross-Sections

The variationally obtained T -matrix elements provide the dynamical information necessary to construct total and differential scattering cross-sections within the framework of the fixed-nuclei approximation. For *non-polar* targets, when the incident electron energy is large with respect to the rotational energy spacings of the molecule, one is usually justified in ignoring the rotational motion of the target and treating the scattering as that produced by an ensemble of randomly oriented, motionless targets.⁴² Under this assumption, the differential cross-section for exciting a molecule from initial electronic state Γ and vibrational state ν to final states Γ' , ν' can be expressed as:

$$\frac{d\sigma}{d\omega}(\Gamma\nu \rightarrow \Gamma'\nu') = \frac{(4\pi)^2}{k_\Gamma^2} \int \frac{d\alpha d\cos\beta d\gamma}{8\pi^2} |\langle k_{\Gamma'}\nu' | T^{\Gamma\Gamma'} | k_{\Gamma}\nu \rangle|^2, \quad (59)$$

where α , β and γ are the three Euler angles that orient the initial and final wave vectors k_Γ and $k_{\Gamma'}$ with respect to the target. The laboratory scattering angle ω is the angle between k_Γ and $k_{\Gamma'}$. The body-frame T -matrix has the expansion:

$$\begin{aligned} \langle k_{\Gamma'}\nu' | T^{\Gamma\Gamma'} | k_{\Gamma}\nu \rangle &= \sum_{\ell\ell'mm'} i^{\ell-\ell'} Y_{\ell m}(k_\Gamma) Y_{\ell'm'}^*(k_{\Gamma'}) \\ &\times \int \chi_\nu(s) T_{\ell m \ell'm'}^{\Gamma\Gamma'}(s) \chi_{\nu'}(s) ds, \end{aligned} \quad (60)$$

where we have used s to denote the internal vibrational coordinates of the target and the vibrational wave functions are χ_ν and $\chi_{\nu'}$. If we are not interested in the individual vibrational levels and simply wish to obtain total cross-sections associated with a particular electronic transition, we can sum Eq. (59) over the final vibrational levels of the target. If we assume that the electron kinetic energy is large compared to the spacing between vibrational levels, then we can use closure,

$$\sum_{\nu'} \chi_{\nu'}(s) \chi_{\nu'}(s') = \delta(s - s'), \quad (61)$$

to obtain

$$\frac{d\sigma}{d\omega}(\Gamma \rightarrow \Gamma')_{\text{total}} = \int \chi_\nu(s) \frac{d\sigma^{\Gamma\Gamma'}}{d\omega}(s) \chi_\nu(s) ds. \quad (62)$$

Thus, the vibrationally summed cross-section is expressed as the expectation value of the fixed-nuclei cross-section with respect to the initial vibrational state of the target. One frequently approximates this quantity by the value of the fixed-nuclei cross-section obtained at the equilibrium geometry of the target.

The usual procedure for carrying out the angular average required in Eq. (59) is to use Wigner rotation matrices to express the spherical harmonics that appear in Eq. (60) in laboratory frame coordinates, and then carry out the averaging analytically.⁴² For arbitrary polyatomics, we have found it easier to carry out the integrations in Eq. (59) by numerical quadrature, keeping the angle between k_Γ and $k_{\Gamma'}$ fixed. Starting with an initial pair of wave vectors k_{Γ_0} and $k_{\Gamma'_0}$ in the body frame, we can express the wave vectors needed to evaluate the integrand (Eq. (59)) for any set of Euler angles, from the expression⁴³:

$$k_\Gamma(\alpha, \beta, \gamma) = \begin{bmatrix} \cos(\alpha) \cos(\beta) \cos(\gamma) - \sin(\alpha) \sin(\gamma) \\ \sin(\alpha) \cos(\beta) \cos(\gamma) + \cos(\alpha) \sin(\gamma) \\ -\sin(\beta) \cos(\gamma) \\ -\cos(\alpha) \cos(\beta) \sin(\gamma) - \sin(\alpha) \cos(\gamma) & \cos(\alpha) \sin(\beta) \\ -\sin(\alpha) \cos(\beta) \sin(\gamma) + \cos(\alpha) \cos(\gamma) & \sin(\alpha) \sin(\beta) \\ \sin(\beta) \sin(\gamma) & \cos(\beta) \end{bmatrix} k_{\Gamma_0}. \quad (63)$$

This numerical approach allows us to avoid the complex angular momentum algebra necessitated by an analytic formulation, and substantially reduces the complexity of the coding required. As we shall see later, it also allows us to easily carry out the modifications of the fixed-nuclei approach that are necessary in order to study electron collisions with *polar* molecules.

2.8. New Technology for Bound-Free Integrals

We have seen that the appearance of free functions in the trial wave function leads to bound-free and free-free integrals that have no analogue in bound-state structure problems. Because there are no simple analytic formulae for these integrals in molecular problems, we have used separable expansions to eliminate most of these integrals from the variational for-

malism and evaluated those integrals that can't be eliminated by adaptive three-dimensional quadrature.

In Sec. 2.2, we showed that it was not necessary to choose the continuum basis functions in the complex Kohn method to be cut-off Bessel functions, and that a more physically motivated, dynamical basis function is obtained by operating with the free-particle Green's function on a short-ranged "test function." We have recently found⁴⁴ that we can exploit this flexibility and choose the test function so as to simplify the computation of bound-free integrals. Indeed, we will show how the evaluation of these integrals can be reduced to one-dimensional quadrature.

Consider a bound-free Coulomb integral of the form:

$$\langle \eta_\ell b | cd \rangle = \iint d^3r d^3r' \eta_\ell(r) \varphi_b^B(r) \frac{1}{|r - r'|} \varphi_c^C(r') \varphi_d^D(r'), \quad (64)$$

where $\varphi_a^A(r)$, is an arbitrary Cartesian Gaussian function centered at A,

$$\varphi_a^A(r) = (x - A_x)^l (y - A_y)^m (z - A_z)^n e^{-a|r-A|^2}, \quad (65)$$

and η_ℓ is a continuum basis function obtained by operating with the outgoing-wave free-particle Green's function on a short-ranged function:

$$\eta_\ell = N_\ell G_0^+ \varphi_\ell. \quad (66)$$

The normalization constant, N_ℓ , will be specified later. The symmetry properties of this function will be determined by those of the test function, φ_ℓ , since G_0^+ is a spherically symmetric operator. In particular, if φ_ℓ is proportional to a single partial wave and the normalization constant, N_ℓ , is chosen correctly, we have⁴⁵

$$\langle r | \eta_\ell \rangle \underset{r \rightarrow \infty}{\sim} k^{1/2} h_\ell^+(kr) Y_{\ell m}(\hat{r}). \quad (67)$$

In order to evaluate these integrals, it is useful to express the Green's function as the Fourier transform of the free-particle propagator

$$G_0^+ = \lim_{\epsilon \rightarrow 0} \frac{1}{E + i\epsilon - H_0} = \frac{1}{i} \int_0^\infty e^{i(E+i\epsilon)t} e^{-iH_0 t} dt, \quad (68)$$

which, in the coordinate representation, takes the form⁴⁶

$$\langle r | e^{-iH_0 t} | r' \rangle = \frac{1}{2\pi i t^{3/2}} e^{(i|r-r'|^2)/(2t)}. \quad (69)$$

Because the other functions in the integrand in Eq. (64) are Gaussians, we choose the test function, φ_ℓ , to be a Gaussian as well. For the moment, let us say that the test function is an *s*-type Gaussian,

$$\varphi_0 = e^{-ar^2}. \quad (70)$$

For this simple case, the integral resulting from operation with the free-particle propagator can be evaluated by elementary means to give

$$\begin{aligned} \langle r | e^{-iH_0 t} | \varphi_0 \rangle &= \frac{1}{2\pi i t^{3/2}} \int e^{(i|r-r'|^2)/(2t)} e^{-ar'^2} d^3r' \\ &= e^{-a_t r^2 + \gamma_t}, \end{aligned} \quad (71)$$

with

$$\begin{aligned} a_t &= a/(1 + 2iat), \\ \gamma_t &= -(3/2) \ln(1 + 2iat). \end{aligned} \quad (72)$$

Since a simple Gaussian function remains Gaussian under the action of the free-particle propagator (spreading in this case but not moving), we can immediately use this fact in combination with Eqs. (64), (66) and (68) to obtain a remarkably simple result for the bound-free two-electron integral

$$\begin{aligned} \langle \eta_\ell b | cd \rangle &= \frac{N_0}{i} \int_0^\infty e^{iEt + \gamma_t} \left[\iint d^3r d^3r' e^{-a_t r^2} \varphi_b^B(r) \frac{1}{|r - r'|} \varphi_c^C(r') \varphi_d^D(r') \right] dt. \end{aligned} \quad (73)$$

This result is remarkable because the integral in the square brackets in Eq. (73) has the form of an ordinary two-electron Gaussian integral. This means we can employ standard electronic structure methods to evaluate this integral.⁴⁷ An appealing interpretation of Eq. (73) is that the continuum function is represented by a spreading Gaussian wave packet, and that the interaction integral for fixed energy is found by Fourier transforming the time-dependent interaction integral involving the wave packet.

The simplicity of this result for *s*-wave bound-free integrals would be useless without a similarly straightforward generalization for higher angular momenta, to which we now turn our attention. Consider the case where

the test function, φ_ℓ , is chosen to be a linear combination of Cartesian Gaussian functions

$$\varphi_\ell = \sum_{i,j,k=0}^{\ell} c_{ijk}^{\ell} x^i y^j z^k e^{-ar^2}. \quad (74)$$

The coefficients c_{ijk}^{ℓ} , can always be chosen so the test function is proportional to a single spherical harmonic, in which case the powers of x , y , and z satisfy

$$i + j + k = \ell, \quad (75)$$

so that with the coefficients chosen appropriately we have a Gaussian proportional to a single spherical harmonic which is also proportional to r^ℓ ,

$$\varphi_\ell = r^\ell e^{-ar^2} Y_{lm}(\hat{r}). \quad (76)$$

The simple result expressed in Eq. (71) suggests that, in the case of a higher angular momentum test function, we look for a solution of the form

$$\langle r | e^{-iH_0 t} | \varphi_\ell \rangle = r^\ell e^{-ar^2 + \gamma_t} Y_{lm}(\hat{r}). \quad (77)$$

We can determine a_t and γ_t by substituting the right hand side of Eq. (77) into the time-dependent Schrödinger equation,

$$i \frac{\partial}{\partial t} r^\ell e^{-a_t r^2 + \gamma_t} = \left[-\frac{1}{2} \frac{1}{r^2} \frac{\partial}{\partial r} r^2 \frac{\partial}{\partial r} + \frac{\ell(\ell+1)}{2r^2} \right] r^\ell e^{-a_t r^2 + \gamma_t}, \quad (78)$$

to get

$$(-i\dot{a}_t r^{\ell+2} + i\dot{\gamma}_t r^\ell) e^{-a_t r^2 + \gamma_t} = (-2a_t^2 r^{\ell+2} + a_t(2\ell+3)r^\ell) e^{-a_t r^2 + \gamma_t}. \quad (79)$$

By equating the coefficients of like powers of r , we obtain the equations

$$\dot{a}_t = -2ia_t^2, \quad \dot{\gamma}_t = -i(2\ell+3)a_t, \quad (80)$$

which have solutions

$$a_t = a/(1+2iat), \quad \gamma_t = -\left(\frac{2\ell+3}{2}\right) \ln(1+2iat). \quad (81)$$

We have thus established the result that

$$\langle r | \eta_\ell \rangle = \langle r | G_0^+ | \varphi_\ell \rangle = N_\ell \sum_{\substack{i,j,k=0 \\ i+j+k=\ell}}^{\ell} c_{ijk}^{\ell} x^i y^j z^k \frac{1}{i} \int_0^\infty e^{iEt} e^{-a_t r^2 + \gamma_t} dt, \quad (82)$$

i.e., that the function obtained by operating with the free-particle Green's function on a Gaussian proportional to single spherical harmonic can itself be expressed as the Fourier transform of a Gaussian with a time-dependent exponent, a_t , and a non-trivial phase provided by the coefficient γ_t . This result allows us to generalize Eq. (73) for an arbitrary angular momentum of the continuum function,

$$\begin{aligned} \langle \eta_\ell b || cd \rangle &= N_\ell \frac{1}{i} \int_0^\infty e^{iEt + \gamma_t} dt \sum_{\substack{i,j,k=0 \\ i+j+k=\ell}}^{\ell} c_{ijk}^{\ell} \\ &\times \left[\iint d^3r d^3r' x^i y^j z^k e^{-a_t r^2} \varphi_b^B(r) \frac{1}{|r-r'|} \varphi_c^C(r') \varphi_d^D(r') \right]. \end{aligned} \quad (83)$$

This result shares the property of the s -wave formula, in that it consists of the Fourier transform of Gaussian two-electron integrals. Again, one of the Gaussians is a spreading wave packet.

The normalization constant, N_ℓ , specified in Eq. (66) is determined by the requirement that the continuum basis function we seek, η_ℓ , behave asymptotically as a purely outgoing partial wave, i.e., that it satisfy Eq. (67). By using the partial wave expansion of the free-particle Green's function²⁹

$$G_0^+(r, r') = -2k \sum_{\ell,m} Y_{\ell m}^*(\hat{r}) Y_{\ell m}(\hat{r}') j_\ell(kr<) h_\ell^+(kr>), \quad (84)$$

along with the defining Eqs. (66), (76) and (84), we find that the normalization constant is given by

$$N_\ell^{-1} = -2\sqrt{k} \int_0^\infty r^{\ell+2} j_\ell(kr) e^{-ar^2} dr. \quad (85)$$

This completes the specification of the continuum basis functions.

By using the representation of $\eta_\ell(r)$ we have derived, we have expressed the general bound-free two-electron integral as the Fourier transform of a

sum of four-center integrals over Gaussian functions, one of which has a time-dependent, complex orbital exponent. Since these integrals can easily be evaluated by modifying the algorithms that are contained in standard molecular integral codes, the entire evaluation of bound-free exchange integrals can be reduced to one-dimensional numerical quadrature. For example, we have found that the McMurchie-Davidson algorithm⁴³ is well suited to the task at hand and we have adopted this approach to efficiently code the complex bound-free integrals needed in a complex Kohn calculation. The choice of points for the one-dimensional time quadrature in Eq. (83) requires some care, because the integrand can be shown to fall off only as $t^{-3/2}$ for large times. Moreover, the integrand can be shown to be analytic except on the positive imaginary t -axis.⁴⁴ Therefore, we can make the integrand fall off exponentially for large t by rotating the integration contour into the upper half t -plane. For example, we can evaluate Eq. (83) as (see Fig. 2)

$$\langle \eta_0 b \| cd \rangle = \frac{N_0}{i} \lim_{T \rightarrow \infty} \int_0^1 dt + \int_1^{T e^{i\theta}} dt e^{iEt + \gamma_t} \\ \times \left[\iint d^3r d^3r' \eta_0(r) \varphi_b^B(r) \frac{1}{|r - r'|} \varphi_c^C(r') \varphi_d^D(r') \right]. \quad (86)$$

The first part of the integration path ($0 \leq t \leq 1$) is kept real, to avoid large gradients coming from singularities in the integrand at small positive imaginary values of t . We have found that, with the rotation angle chosen in the range from 30° to 45° , we can accurately evaluate the bound-free Coulomb integrals over a wide range of Gaussian exponents with roughly fifty time points.

The consequence of these developments is that it may not be necessary to use primitive separable approximations to simplify the evaluation of bound-free exchange integrals. Another, possibly more important, consequence is that we will not have to project the optical potential on to a basis to simplify its evaluation. Recall that we have defined V_{opt} as

$$V_{\text{opt}} = \mathbf{PHQ} \left[\frac{1}{E - \mathbf{QHQ}} \right] \mathbf{QHP}. \quad (87)$$

By its definition, \mathbf{Q} projects on a space of exponentially bounded functions and can be constructed in a molecular calculation from many-electron functions involving only Gaussians. Therefore, free-free matrix elements of

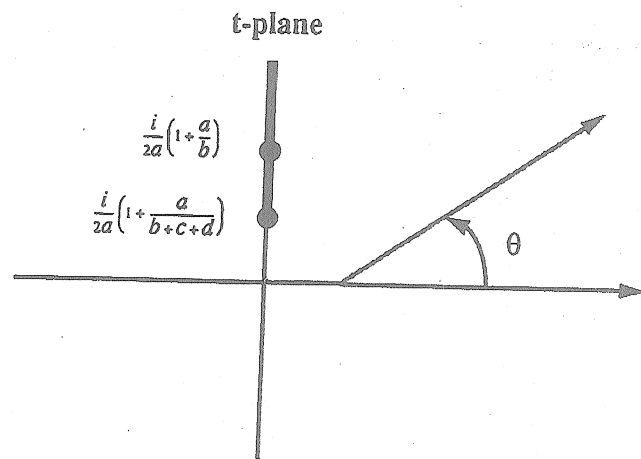


Fig. 2. Analytic structure of integrand in Eq. (86). There is a simple pole and a branch point on the positive imaginary t -axis.

V_{opt} involve only bound-free and bound-bound matrix elements of the Hamiltonian.

A completely analytic approach requires a procedure for computing free-free exchange integrals. The generalization of the procedure just outlined would require a two-dimensional quadrature over complex Gaussian matrix elements, which is not practical at this point. An alternative is to use, just for the exchange interactions,⁴⁹ a separable expansion of the form

$$V^N = \sum_{\alpha, \beta=1}^N V|\alpha\rangle d_{\alpha, \beta}^N \langle \beta|V, \quad (88)$$

where

$$[d^{-1}]_{\alpha, \beta} = \sum_{\alpha, \beta=1}^N \langle \alpha|V|\beta\rangle, \quad (89)$$

and only short-ranged functions are employed in the sums. This approximation, which forms the basis of the Schwinger variational method,⁵⁰ is known to converge more rapidly than the primitive separable form given in Eq. (45).⁵¹ The use of Eq. (88) for exchange interactions requires only bound-free integrals for its implementation.

We have already seen in several preliminary applications that the ideas presented here allow for the use of much smaller expansion basis sets than

have previously been employed. These preliminary tests, however, have only been carried out at the static-exchange level with simple closed-shell target wave functions. The full incorporation of this new complex integral technology into our structure and scattering codes is a task that is presently under way.

3. Aspects of the Close-Coupling Method

This discussion has focused on the mechanical details of how the matrix equations of the complex Kohn variational method are set up. The foregoing discussion makes it clear that the formulation admits the use of multiconfiguration target wave functions and large-scale optical potentials, and that modern electronic structure techniques can be used to carry out most of the manipulations required quite efficiently. We wish to emphasize, however, that the partitioning of P -space and Q -space terms, and the appropriateness of certain configurations, is ultimately dictated by physical consideration of the underlying approximations.

3.1. The Close-Coupling Plus Correlation Method

The close-coupling formalism, in which N -electron target states are used as a basis for expanding the full $(N + 1)$ -electron wave function, is central to many *ab initio* scattering approaches. In applying this formalism, we are confronted with two problems. First, there is the obvious difficulty that, as the incident energy in a collision is increased toward the ionization energy, the number of open channels approaches infinity. Practical considerations thus generally limit the number of target states that can be included in a close-coupling calculation. Even if one is only interested in cross-sections for excitation to low-lying excited states and can use physical considerations as a guide in determining which excited states should be explicitly included in the close-coupling expansion, the excitation cross-sections may be needed at energies well above the thresholds of other low-lying states. It is, therefore, natural to inquire about the effect of neglected channels at intermediate collision energies and to examine whether there is anything about the close-coupling formulation that might lead to pathological results.

A second problem is that, with the exception of single-electron atoms and ions, exact target states are not known and approximate wave functions must be used. These are generally expressed as linear combinations of configuration state functions built from a specified list of "target" orbitals.

To simplify the formulation of the collision problem and the evaluation of many-electron matrix elements, we have followed the standard practice of requiring the scattering functions to be orthogonal to all of the target orbitals.⁵²⁻⁵⁴ It is well known that this strong orthogonality constraint can lead to physically incorrect results if it is not relaxed. Indeed, early calculations on electron impact dissociation of H_2 (Refs. 6 and 55) were subsequently shown to be incorrect for precisely this reason. We have also noted that the standard remedy for removing this constraint is to include in the wave function $(N + 1)$ -electron penetration terms which are built exclusively from target orbitals by taking the direct product of the target orbitals and all the N -electron configurations used in building the target wave functions. One then retains all such terms that are consistent with the Pauli exclusion principle and that have the same symmetry as the total wave function. We shall refer to methods which use this type of wave function as close-coupling plus correlation (CCPC) methods. The trial function defined in Eq. (29) is typical of this approach. As we shall see, both of the problems just mentioned can lead to problems that are symptomatic of the same disease.

The CCPC approach is well suited to low energy electron scattering calculations where one can explicitly retain all open electronic channels in the trial wave function. The CCPC wave function can then be used to systematically study the effects of target polarization and to study the cross-sections in threshold regions that may be dominated by Feshbach resonances (doubly-excited states). We have used this approach in the case of $e^- + Li_2$ scattering,⁵⁶ and will illustrate the results of that study below.

3.2. The Multiconfiguration Close-Coupling Method

With a CCPC wave function, the coefficients of the individual penetration terms are chosen variationally. This procedure can, in the case of multiconfiguration target states, provide more flexibility than the minimum needed to compensate for any orthogonality constraints, and can actually incorporate additional correlation effects.⁵⁷ In effect, the penetration terms built from N -electron configurations that contribute weakly to the target states explicitly chosen can represent excited pseudo-states and can give rise to broad, unphysical resonances at intermediate energies where no structure is expected.

We can illustrate this phenomenon with the simple example of elastic scattering of an electron from H_2 in $^2\Sigma_g^+$ symmetry. For the ground-state $X^1\Sigma_g^+$ wave function, we use a simple configuration-interaction wave function of the form $(C_1 1\sigma_g^2 + C_2 1\sigma_u^2)$, with $C_1 = 0.9968$ and $C_2 = 0.0799$. In this case we need a single penetration term $1\sigma_u^2 1\sigma_g$ in the trial wave function to relax the orthogonality constraint on the scattering wave function with respect to the $1\sigma_g$ orbital. The complex Kohn method was used to solve for the elastic cross-section. The result is shown in Fig. 3. There is evidently a broad resonance near 16 eV. Elastic scattering cross-sections obtained with a simple self-consistent field (SCF) target wave function, which differs only slightly from the target CI wave function we used, show no such structure. Moreover, if the calculation is performed without the $1\sigma_u^2 1\sigma_g$ term, the resonance disappears. This result is also shown in Fig. 3.

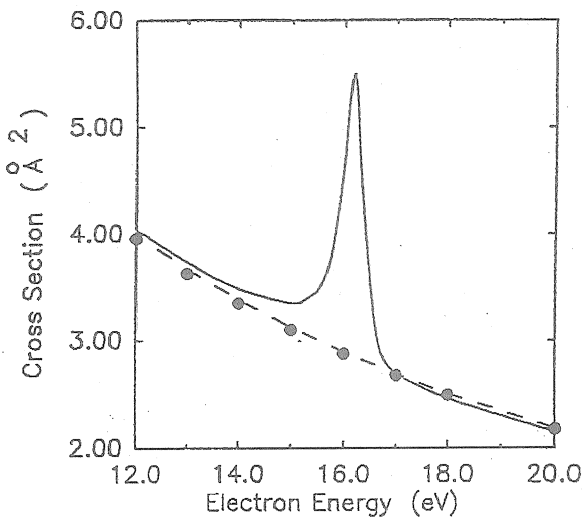


Fig. 3. $e^- + H_2 \Sigma_g^+$ elastic cross-section. Solid curve, static-exchange plus penetration term; dashed curve, static-exchange without penetration term; circles, two-channel calculation including penetration term.

The $1\sigma_u^2 1\sigma_g$ term can be thought of as a doubly excited negative ion term whose parent is the $(1\sigma_g 1\sigma_u), b^3\Sigma_u^+$ state of H_2 . This state is physically open at energies above 10 eV, but is not properly included in the

single-channel calculation. To demonstrate this, we performed a third calculation in which the $X^1\Sigma_g^+$ and $b^3\Sigma_u^+$ states were both included in the open channel portion of the trial function and the single penetration term was again retained. The resulting elastic cross-section, shown in Fig. 3, is evidently quite close to the smooth result obtained from the single-channel calculations in which the penetration term was dropped. This simple example serves to show how excited states, which are not explicitly included in the close-coupling expansion, can enter the problem in an indirect way when correlated target wave functions are used. In this simple case, it is possible to easily identify the cause of the trouble and remove the term responsible for this behavior from the single-channel trial function.

We have shown that it is possible to develop a procedure for incorporating the penetration terms in the expansion of the total wave function in fixed linear combinations that are consistent with the approximate target states that are being employed.⁵⁷ This contraction of the Hilbert space component of the total wave function then allows us to develop a procedure for identifying and eliminating the terms in the trial wave function that will give rise to pseudo-resonances. This procedure effectively allows one to meaningfully apply the close-coupling method at intermediate energies even when elaborate multi-reference target states are employed. Instead of the general CCPC expansion, we introduce a multiconfiguration close-coupling (MCCC) expansion of the total wave function, where the terms comprising Q -space are restricted to the penetration terms which arise by taking the direct product of the target wave function and occupied orbitals.

$$\begin{aligned}
 \Psi_{\Gamma} &= \sum_{\Gamma'} A(\chi_{\Gamma'} F_{\Gamma\Gamma'}) + \sum_{\Gamma'\sigma} d_{\sigma}^{\Gamma\Gamma'} A(\chi_{\Gamma'} \varphi_{\sigma}) \\
 &= \sum_{\Gamma'} A(\chi_{\Gamma'} F_{\Gamma\Gamma'}) + \sum_{\Gamma'\sigma} d_{\sigma}^{\Gamma\Gamma'} \sum_{\mu} T_{\sigma\mu}^{\Gamma'} \Theta_{\mu} \\
 &= \sum_{\Gamma'} A(\chi_{\Gamma'} F_{\Gamma\Gamma'}) + \sum_{\Gamma'\sigma} d_{\sigma}^{\Gamma\Gamma'} \omega_{\sigma}^{\Gamma'}.
 \end{aligned} \quad (90)$$

Thus there will be one Q -space term for each partially occupied orbital in the target wave function $\chi_{\Gamma'}$ (the product $A(\chi_{\Gamma'} \varphi_{\sigma})$ vanishes if φ_{σ} is doubly occupied in every CSF used in the expansion of $\chi_{\Gamma'}$). The Q -space configurations, Θ_{μ} , used in a CCPC expansion are generated by taking the direct product of an occupied orbital and every CSF appearing in the

target wave function, whereas the Q -space terms appearing in the MCCC wave function are the direct product of occupied orbitals and the linear combination of CSF's which define the target states. Thus, penetration terms which appear in the multiconfiguration close-coupling wave function can be expressed as a contraction of the Q -space terms in the CCPC trial function.

While it is a simple matter to build the list of $(N + 1)$ -electron CSF's, Θ_μ , needed in the CCPC wave function which are consistent with the Pauli exclusion principle, the construction of the transformation matrix, $T_{\sigma\mu}^t$, used to build the Q -space CSF's employed in the MCCC wave function requires some additional effort. However the construction of these terms is neither a formal nor a computational problem of note. In fact, this matrix can be constructed by modifying the transition density code present in most modern electronic structure packages. The (non-square) transformation matrix we need to contract the Q -space configurations which appear in the trial scattering function can be easily constructed if we expand the CSF's in terms of determinants, but a more efficient scheme is desired if we wish to exploit the power of the current generation of electronic-structure codes.

We need consider only that portion of the trial scattering function which gives rise to penetration terms in the MCCC method,

$$\Psi_t = A(\chi_t(N)f(N+1)), \quad (91)$$

where the one-electron scattering function is now expanded only in terms of occupied orbitals, $f = \sum_\sigma C_\sigma \varphi_\sigma$. We can rewrite this portion of the trial scattering function as

$$\Psi_t = \sum_\sigma C_\sigma \sum_\mu T_{\mu\sigma} \Theta_\mu(N+1), \quad (92)$$

where we now have a sum over antisymmetric $(N+1)$ -electron configuration state functions. To obtain elements of the transformation matrix $T_{\mu\sigma}$, we only need consider the contributions from one of the occupied orbitals,

$$T_{\mu\sigma} = \langle A(\chi_t \varphi_\sigma) | \Theta_\mu \rangle. \quad (93)$$

This matrix element is obtained by replacing the occupied orbital φ_σ from the one-electron scattering function, f , with an arbitrary scattering orbital

φ_s . This arbitrary scattering orbital is orthogonal to all of the occupied orbitals and is used to represent the one-electron scattering function, f , in the computation of the transition density matrix that we will use to construct the $T_{\mu\sigma}$ transformation matrix. We then compute the one-particle transition density matrix between these functions

$$\begin{aligned} d^\mu(1, 1') &= \langle \Theta_\mu | A(\chi_t \varphi_s) \rangle_1 \\ &\equiv \int \Theta_\mu(1 \dots N+1) A(\chi_t(1' \dots N) \varphi_s(N+1)) d2 \dots dN + 1. \end{aligned} \quad (94)$$

The nonzero matrix elements of this density must involve the scattering orbital φ_s , since none of the $(N+1)$ -electron CSF's comprising Q -space, Θ_μ , contain this orbital. Thus, the only nonzero terms in this matrix are of the form $d_{\sigma,s}^\mu$. We will show that these density matrix elements are components of the transformation matrix we need to contract Q -space, that is,

$$T_{\mu\sigma} = d_{\sigma,s}^\mu. \quad (95)$$

In order to obtain a nonzero overlap between a Q -space configuration state function, Θ_μ , and the target wave function, the trace of the density defined in Eq. (94) must be nonzero. This means a nonzero overlap of these functions will result if the prototype scattering orbital, φ_s , is replaced by the occupied orbital φ_σ in the direct product wave function. This can be easily seen by expanding the CSF's used to build the target wave function and the Q -space CSF's in terms of determinants. Now consider what occurs on a determinant-by-determinant basis when we construct a direct product wave function as a target determinant $\Phi_t = A \varphi_1^\alpha \varphi_2^\beta \varphi_3^\gamma$ times a target orbital. If the direct product function does not violate the Pauli principle, then the overlap can be only 1, -1 or 0 with a Q -space determinant. Consider the example

$$\begin{aligned} A(\Phi_t \varphi_3^\alpha) &\equiv A(\varphi_1^\alpha \varphi_2^\alpha \varphi_3^\beta \varphi_3^\alpha) \\ &\equiv \Theta_1, \end{aligned} \quad (96)$$

and the density matrix which results when the occupied orbital φ_3^α is replaced by a scattering orbital φ_s^α ,

$$\langle A \Phi_t \varphi_s^\alpha | \Theta_1 \rangle_1 = |\varphi_s^\alpha \rangle \langle \varphi_3^\alpha|. \quad (97)$$

In this case the matrix element, d_{3s}^1 , is 1. Now if we consider another Q -space determinant

$$\Theta_2 = A\varphi_1^\alpha\varphi_2^\alpha\varphi_2^\beta\varphi_3^\alpha, \quad (98)$$

then a zero matrix element would ensue:

$$\langle A\Phi_t\varphi_s^\alpha || \Theta_2 \rangle_1 = 0, \quad (99)$$

which is again the desired result. Since a phase factor in the overlap results in the same phase factor in the density, these are the only two cases we need consider. Because we can expand a wave function expressed in terms of CSF's as one expanded in terms of determinants, the fact that each determinant-determinant interaction is treated correctly means that we can obtain the desired transformation matrix, $T_{\mu\sigma}$, by computing density matrix elements between CSF's.

3.3. Intermediate Energy Scattering

The basic idea underlying the close-coupling method is that the set of target states included in the expansion of the total wave function can be extended toward completeness. In practice, the expansion must be severely truncated so that physical considerations must dictate which target states to include. One consequence of this truncation, as noted previously, is that spurious resonances can arise in the cross-sections obtained in CCPC calculations as a consequence of excluding certain open channels from the close-coupling expansion. The consequence of truncating the CCPC expansion is that there may be terms in Q -space which are the direct product of major components of missing open-channel wave functions and occupied orbitals. These terms can be identified with eigenvalues of the Q -space Hamiltonian, which give rise to spurious resonances. The contraction of Q -space inherent in the MCCC Hamiltonian eliminates most, but not all, of these spurious poles. In order to understand the type of terms which arise by contracting Q -space, consider a single-channel (static-exchange) calculation, which employs the following target wave function:

$$\chi = C_1 A\varphi_1^2 + C_2 A\{\varphi_2\varphi_3\}_{\text{singlet}}, \quad (100)$$

where $C_1 \cong 0.9$ and $C_2 \cong 0.4$. Then the unnormalized Q -space CSF's would be

$$\begin{aligned} \omega_1 &= C_2 A\varphi_1\{\varphi_2\varphi_3\}_{\text{singlet}}, \\ \omega_2 &= C_1 A\varphi_1^2\varphi_2 - \frac{1}{\sqrt{2}}C_2 A\varphi_2^2\varphi_3, \\ \omega_3 &= C_1 A\varphi_1^2\varphi_3 - \frac{1}{\sqrt{2}}C_2 A\varphi_2\varphi_3^2. \end{aligned} \quad (101)$$

The direct product of the strongly occupied orbital, φ_1 , with the target wave function can be associated with an excited state whose principal CSF is $\varphi_2\varphi_3$ while the direct products of the weakly occupied orbitals, φ_2 and φ_3 , and the target wave function give rise to Q -space CSF's associated with the target wave function itself. The norm of these direct product CSF's also reflects this dichotomy of terms. The terms associated with the target wave function have norms which are close to one, while the term associated with an excited state will have a norm close to zero. The excited state terms which lead to spurious resonances are now easily identified and can be removed from Q -space.

This procedure is based upon the notion that the excited states, associated with the small components of the physical states included, are not strongly coupled to those states which have been included in the trial function. We wish to emphasize that we are not now referring to spectroscopic states of the target which may have physical resonances associated with their thresholds, but rather the broad structures generated by pseudo-states that occur at energies above the ionization threshold of the target, where no such behavior is expected. One can test this procedure by performing CCPC calculations at low incident electron energies, where all of the penetration terms can be included in the problem, and comparing the results to MCCC calculations with and without terms being excluded from Q -space.

A note about the target orbitals bears further comment. In the examples we have considered, the target wave functions are assumed to have a compact representation in terms of the orbital set chosen so that it is easy to identify a principal configuration for each target state. However, it is not always possible to achieve a compact representation of the ground and excited states using a single orbital set. This may be the case with excited

states that have mixed valence-Rydberg character, such as the B -state of H_2 . In such instances our prescription for identifying excited pseudo-states, which is based on the norm of a contracted $(N+1)$ -electron function, might fail. The remedy for this problem is to carry out a rotation of the target orbitals, on a state by state basis, to obtain the desired representation of the ω -basis. For each target state in the scattering calculation, these orbitals can be chosen so as to extremize the norm of the contracted $(N+1)$ -electron functions. We can simply form the overlap matrix for the set of ω -vectors generated by a particular target state and diagonalize it. This procedure then defines a new transformation of the contracted Q -space Hamiltonian. We note that this transformation does not introduce any additional complexities into the construction of the optical potential, since the linear combinations of $(N+1)$ -electron CSF's comprising the ω basis are not, in general, orthogonal.

This transformation provides a unique definition of these contracted functions which is independent of the orbital basis used to define the target wave functions and guarantees that the MCCC results will not depend on the way in which the target orbitals are defined.

4. Long-Range Interactions

In electron collision problems, special care is needed in cases where the scattering is dominated by long-range interactions. An obvious special case is electron scattering by an ionic target. Since the addition of a Coulomb potential to any short-ranged potential results in an interaction which displays the characteristic slow decrease of the Coulomb field, appropriate steps must be taken to develop a proper formalism to handle this case.⁵⁸ In particular, the asymptotic form of the free functions we have assumed for scattering by neutral targets must be appropriately modified. The solution in this case is to split the Coulomb term off from the rest of the interaction and to express the T -matrix as a sum of the pure Coulomb T -matrix and a distorted wave T -matrix which describes the scattering by the residual interaction (i.e., the interaction less the Coulomb potential) and is defined just like T , except that the free particle functions are replaced by Coulomb functions. This is a straightforward application of the two-potential formalism.⁵⁹ Complex Kohn variational calculations for electron scattering by several molecular ions have been reported using this distorted wave formalism.^{31,60}

4.1. Dipole Interactions

The case of the dipole interaction is a bit more subtle and warrants explanation in some detail. One encounters this interaction when calculating excitation cross-sections between optically allowed states. For such dipole-allowed transitions, many partial-wave components are needed to properly describe scattering for small deflection angles of the incident electron and to obtain converged total cross-sections. The reason is that the underlying direct transition potential for such transitions gives rise to a long-range interaction which behaves asymptotically as $D \cdot r/r^3$, where D is the transition dipole moment. It is neither possible nor necessary, however, to carry the full complement of partial waves in a coupled-channel variational calculation to obtain converged cross-sections. Beyond a certain ℓ cutoff, the partial-wave components of the scattering functions do not penetrate the interior part of the molecular target. In this weak scattering limit, it is sufficient to employ a perturbative treatment such as the Born approximation. In fact, a useful strategy is to expand the difference between a desired quantity and its value in the first Born approximation as a rapidly convergent partial-wave series and then to use a completion formula to obtain the final result.^{61,62}

One also encounters the dipole interaction in electronically elastic scattering of electrons by molecules that have a permanent dipole moment.⁶³ In such cases, one has the additional *formal* difficulty that a fixed-nuclei treatment of electron scattering by a polar molecule gives infinite total cross-sections and differential cross-sections that diverge at zero scattering angle.⁶⁴ This essential property of the dipole potential can usually be remedied by introducing the rotational motion of the target molecule.^{64,65} The strategy again is to use a hybrid treatment in which only the low order partial-wave components of the T -matrix are determined from variational calculations and the higher order terms are included in the Born approximation via a closure formula. However, in this case the use of closure is more than a matter of computational convenience.⁶⁶ It is formally necessary since, as we will show, the partial-wave expansion of the *body-fixed* T -matrix obtained in the adiabatic nuclei approximation diverges at all scattering angles.

The partial-wave Born approximation for a particular T -matrix element contributing to a dipole-allowed process $\Gamma \rightarrow \Gamma'$ is given by

$${}^B T_{\ell m \ell' m'}^{\Gamma \Gamma'} = 2\sqrt{k_\Gamma k_{\Gamma'}} \int j_{\ell'}(k_{\Gamma'} r) Y_{\ell' m'}^*(\hat{r}) (\chi_\Gamma H \chi_{\Gamma'}) j_\ell(k_\Gamma r) Y_{\ell m}(\hat{r}) d^3 r. \quad (102)$$

Consistent with this approximation is the replacement of $(\chi_\Gamma H \chi_{\Gamma'})$ by its asymptotic form⁶⁷:

$$\begin{aligned} V_{\Gamma \Gamma'}(r) &= (\chi_\Gamma H \chi_{\Gamma'}) \\ &\equiv \int \chi_\Gamma(r_1, \dots, r_N) H(r, r_1, \dots, r_N) \chi_{\Gamma'}(r_1, \dots, r_N) dr_1 \dots dr_N \\ &\sim D \cdot \hat{r}/r^2, \end{aligned} \quad (103)$$

where D is the transition moment (or, when $\Gamma = \Gamma'$, the permanent dipole moment) and \hat{r} is a unit vector in the body frame of the molecule. With this limiting form of the potential, the first Born approximation gives extremely simple formulae for scattering amplitudes and cross-sections that can serve as a useful starting point for a more elaborate treatment of the dynamics. For example, the full body-frame, fixed-nuclei T -matrix is given as⁶⁴:

$$\begin{aligned} \langle k_{\Gamma'} | {}^B T^{\Gamma \Gamma'} | k_\Gamma \rangle &= -\frac{\sqrt{k_\Gamma k_{\Gamma'}}}{8\pi^2} \int e^{-i(k_{\Gamma'} - k_\Gamma) \cdot r} \left(\frac{D \cdot \hat{r}}{r^2} \right) d^3 r \\ &= -\frac{\sqrt{k_\Gamma k_{\Gamma'}} i D \cdot \hat{k}'}{2\pi |k_\Gamma - k_{\Gamma'}|}, \end{aligned} \quad (104)$$

where $\hat{k}' = (k_{\Gamma'} - k_\Gamma)/|k_{\Gamma'} - k_\Gamma|$. We now write the partial wave expansion of the exact body frame T -matrix in the following form:

$$\begin{aligned} \langle k_\Gamma | T^{\Gamma \Gamma'} | k_{\Gamma'} \rangle &= -\frac{\sqrt{k_\Gamma k_{\Gamma'}} i D \cdot \hat{k}'}{2\pi^2 |k_\Gamma - k_{\Gamma'}|} \\ &+ \sum_{\substack{\ell' \ell \\ m' m}} i^{\ell - \ell'} Y_{\ell' m'}^*(\hat{k}_{\Gamma'}) Y_{\ell m}(\hat{k}_\Gamma) (T_{\ell m \ell' m'}^{\Gamma \Gamma'} - {}^B T_{\ell m \ell' m'}^{\Gamma \Gamma'}), \end{aligned} \quad (105)$$

where we have merely added and subtracted the Born approximation to the partial wave expansion of the exact T -matrix. The point to note is that the sum in Eq. (105) now contains differences between exact and Born partial wave elements, which rapidly approach zero as $\ell(\ell')$ gets large. To obtain

converged cross-sections, we need only compute variational T -matrix elements to high enough ℓ , where the Born approximation is accurate. Note that it is essential to employ a consistent phase convention in evaluating the various contributions to Eq. (105). It is also necessary to define the transition moment D used in the Born approximation to the T -matrix in the same coordinate system that is used in the electronic structure calculation. To obtain differential (and total) cross-sections corresponding to a random orientation of the target molecule with respect to an incident electron beam in the laboratory frame, we simply substitute the amplitude defined in Eq. (105) into Eq. (59) and carry out the average over molecular orientations numerically, as explained in Sec. 2.7.

For electronically elastic scattering by a polar molecule, the fixed-nuclei approach gives, as we have said, infinite total cross-sections and a differential cross-section that diverges in the forward direction. This is an essential property of the space-fixed dipole potential and not just a result of using the Born approximation. However, even though the adiabatic approximation⁶⁸ cannot be directly used to obtain total cross-sections for polar molecules, Eq. (105) is nevertheless perfectly adequate for studying scattering out of the forward direction and for calculating momentum transfer cross-sections, which are insensitive to the form of the differential cross-section near zero degrees, as long as the electron energy is large compared to the spacing of the rotational levels.⁶³

To compute total cross-sections for polar molecules, we must introduce the rotational motion of the target. This is most easily accomplished by treating the molecule as a rigid rotor and adding the rotational Hamiltonian to the total Hamiltonian that is used to describe the electron-plus-target system.⁶⁹ However, the fixed-nuclei approximation, in which the rotational Hamiltonian is neglected in a body-frame formulation of the collision problem, leads to substantial simplifications in the dynamics compared to corresponding space-fixed frame calculations. Fully coupled laboratory frame calculations are only feasible when model potentials are used. Virtually all *ab initio* calculations on electron-molecule scattering have been carried out in the fixed-nuclei approximation. If we wish to obtain total cross-sections for polar molecules, we can use the hybrid approach of Padial and Norcross⁷⁰ when applying Born closure: for the rapidly converging differences between partial-wave T -matrix elements, we use fixed-nuclei quantities, but include rotational quantum numbers in the full Born amplitude. This is justified because, as Collins and Norcross⁶³ have demonstrated, for

low angular momentum quantum numbers, the differences in the T -matrix elements obtained from lab-frame calculations and frame-transformed fixed-nuclei calculations are insignificant for polar targets.

The Born approximation for a rotating point dipole still has a simple analytic form. If we denote the rotor eigenfunctions as $\mathcal{Y}_{qJM}(s)$ where J and M label, respectively, the magnitude of the molecular angular momentum and its projection on the axis of quantization, q represents any other quantum numbers necessary to specify a non-linear target and s is the set of internal rotor coordinates, then we can write the differential cross-section (after summing over M' and averaging over M) for the process ($qJ \rightarrow q'J'$) produced by the point dipole interaction in the first Born approximation⁷¹:

$$\begin{aligned} \frac{d\sigma^{\text{Born}}}{d\omega}(qJ \rightarrow q'J') &= \left(\frac{1}{2\pi}\right)^2 \frac{D^2}{2J+1} \frac{k'}{k} \\ &\times \sum_{MM'} \left| \int \frac{e^{i(\mathbf{k}'-\mathbf{k}) \cdot \mathbf{r}}}{r^2} \mathcal{Y}_{q'J'M'}(s) \hat{\mathbf{r}} \cdot \hat{\mathbf{D}} \mathcal{Y}_{qJM}(s) d^3r ds \right|^2 \\ &= \frac{4}{3} \frac{D^2}{2J+1} \frac{k'}{k} \frac{1}{(k^2 + k'^2 - 2kk' \cos \theta)} |\langle \alpha' J' | c^1 | \alpha J \rangle|^2. \end{aligned} \quad (106)$$

The expression for the reduced matrix element ($\alpha' J' | c^1 | \alpha J \rangle$) will depend on the specific symmetry properties of the target rotor.⁷¹ For example, the rotational eigenfunctions of a simple linear rotor are the spherical harmonics for which we obtain the result

$$\frac{d\sigma^{\text{Born}}}{d\omega}(J \rightarrow J') = \frac{4}{3} \frac{D^2}{|k'-k|^2} \frac{k'}{k} \frac{J}{2J+1} \delta_{J,J' \pm 1}. \quad (107)$$

The initial and final wave vectors are related by

$$k'^2 - k^2 = 2(E_{J'} - E_J), \quad (108)$$

with

$$E_J = \frac{J(J+1)}{2I}, \quad (109)$$

where I is the moment of inertia. Since all the scattering is inelastic, k' and k are never equal, and the cross-section is always finite. We can again use

a closure formula to compute the cross-section for rotational excitation. The amplitude defined in Eq. (105) is simply multiplied by the product of rotational functions, as in Eq. (106), before carrying out the angular average required in Eq. (59). Moreover, in the spirit of the hybrid treatment of Padial and Norcross,⁷⁰ we can ignore the rotational energy splittings in the partial wave sums and use fixed-nuclei quantities for the partial-wave T -matrix elements. The point is that a closure formula like that of Eq. (105) still allows one to obtain results from fixed-nuclei calculations with no significant compromise in accuracy.

Our technique for applying Born-closure and evaluating differential cross-sections differs from the procedures usually employed. When the orientational averaging of the fixed-nuclei cross-section is formulated analytically, the usual procedure is to express the differential cross-section as a Legendre series⁴²:

$$\frac{d\sigma}{d\omega} = \sum_{\lambda=0}^{\infty} A_{\lambda} P_{\lambda}(\cos \theta). \quad (110)$$

For polar targets, the A_{λ} coefficients with large λ get most of their contribution from terms involving T -matrix elements with large ℓ values for which the Born approximation gives good values.^{61,62} Thus the formula

$$\frac{d\sigma}{d\omega} = \frac{d\sigma^{\text{Born}}}{d\omega} + \sum_{\lambda=0}^{\lambda_{\max}} (A_{\lambda} - A_{\lambda}^{\text{Born}}) P_{\lambda}(\cos \theta) \quad (111)$$

can be used to accelerate convergence. We have found however, that Eq. (111) requires higher ℓ -values for convergence than does Eq. (105), since there are interference terms that do not cancel in the sum that appears in Eq. (111) and may not be negligible unless λ is sufficiently large. Indeed, Eq. (111) can actually give negative cross-sections if the angular momentum sums are too severely truncated. This is never the case when closure is applied directly to the scattering amplitude.^{66,72,73}

The use of a closure formula for the amplitude (or the cross-section) in calculations carried out on polar molecules within the fixed-nuclei approximation is more than a numerical device for accelerating convergence. Indeed, it is the case that the partial-wave expansion of the fixed-nuclei amplitude diverges for all values of the scattering angle. This is easily demonstrated for the first Born amplitude (first term in Eq. (105)). Consider a case where the target orientation is such that the dipole moment lies

in the direction of the momentum transfer vector, $\mathbf{k}' - \mathbf{k}$. The fixed-nuclei Born T -matrix is then simply

$$f = \frac{-iD}{2\pi\sqrt{2}} \frac{1}{\sqrt{1 - \cos \theta}}. \quad (112)$$

If we try to expand this in a partial-wave series

$$f = \sum_{\ell} f_{\ell} P_{\ell}(\cos \theta), \quad (113)$$

we obtain⁷⁴

$$\begin{aligned} f_{\ell} &= -\left(\frac{2\ell+1}{2}\right) \frac{iD}{2\pi\sqrt{2}} \int_{-1}^1 \frac{P_{\ell}(x)}{\sqrt{1-x}} dx \\ &= \frac{iD}{2\pi}. \end{aligned} \quad (114)$$

The series given by Eq. (113) is thus non-convergent for all values of θ . The Legendre expansion of the cross-section in this case is also undefined, since the integral $\int_0^\infty P_{\ell}(x)/(1-x)dx$ is infinite. The fact that we have used the first Born values of the scattering amplitude to demonstrate the non-convergence of the partial-wave expansion for the fixed-nuclei T -matrix and/or cross-section does not affect our conclusion that the partial-wave expansions of the corresponding exact fixed-nuclei quantities are also divergent. This behavior is due to the long-range nature of the interaction and the consequent slow fall-off of the partial-wave T -matrix elements for large ℓ .⁶⁵ One often sees the statement that the low partial-wave contributions to the scattering amplitude can nevertheless provide quantitatively meaningful estimates of the differential cross-section out of the forward direction. This is indeed true, but they should be used only in conjunction with a closure formula.

5. Applications

5.1. Polarized-SCF Studies (CH_4 , SiH_4 , C_2H_4 , C_2H_6)

Ramsauer-Townsend minima are a ubiquitous feature in the elastic low-energy electron scattering cross-sections of many small polyatomic molecules. These features were first observed in the elastic cross-sections

of the heavier rare gases,⁷⁵ and their origin is well understood.⁷⁶ With a closed-shell, non-polar target, two effects dominate the low-energy electron scattering. There is an underlying electrostatic interaction between the electron and the target which, because of the exchange interaction between the incident and target electrons, is essentially repulsive at short distances. There is also a longer range polarization interaction caused by the distortion of the charge cloud of the target in the electric field of the incident electron. This interaction is attractive. At a particular energy, these two interactions may effectively cancel and the totally symmetric (s -wave) contribution to the cross-section vanishes. If this occurs at a low enough energy where the higher symmetry contributions are negligible, there will be a pronounced minimum in the elastic cross-section.

For a number of target molecules, including CH_4 , SiH_4 , C_2H_4 and C_2H_6 (Refs. 32, 77, 78 and 79 respectively) we have shown that a near-quantitative description of the low-energy scattering can be achieved by employing a polarized-SCF trial function. At this level, the target ground state is described by an SCF wave function, while the space of closed channels is treated by including single excitations from the ground-state into a small space of polarized orbitals. This simple description of electron correlation in the colliding system was found to provide a consistent treatment of the N - and $(N+1)$ -electron portions of the problem.

The notion of a polarized orbital in scattering calculations is usually associated with the method of Callaway *et al.*⁸⁰ and Temkin and Lamkin.⁸¹ In this approximation, the interaction between the incident electron and the target is treated adiabatically. The response of a Hartree-Fock orbital to an external field is represented as the sum of a Hartree-Fock orbital and a polarized orbital, $\varphi_1 = \varphi_0 + \varphi_p$, which is determined at a number of electron-target separations. These orbitals are then used to define adiabatic static and polarization potentials. In our work, we only use polarized-orbital basis functions to efficiently incorporate target polarization effects into the closed-channel part of the trial wave function ($Q\Psi$).

The expression for a component of the dipole polarizability of an atom or molecule in first order perturbation theory is

$$\alpha_k = 2 \sum_{i \neq 0} \frac{\langle \chi_i | \mu_k | \chi_0 \rangle^2}{E_i - E_0}, \quad (115)$$

where μ_k is a component of the dipole operator, χ_0 is the target wave function and E_0 is its energy. χ_i is an excited state wave function with energy

E_i . If we adopt an independent orbital approximation, where one orbital will be polarized and all of the other orbitals are frozen, this polarizability expression reduces to a simpler form which only requires the construction of one-electron Fock operators,

$$\alpha_{n,k} = 2 \sum_{i \neq n}^{\text{virtual}} \frac{\langle \varphi_i | \mu_k | \varphi_n \rangle^2}{\epsilon_i - \epsilon_n}, \quad (116)$$

where φ_n is the Hartree-Fock (HF) orbital that is being polarized and ϵ_n is its HF eigenvalue. In order to employ this simple polarizability expression, the virtual orbitals must be eigenfunctions of a one-electron V_{N-1} Fock operator. Thus in Eq. (116) φ_n is a singlet-coupled Improved Virtual Orbital⁸² (IVO), an eigenvector of the one-electron IVO or V_{N-1} Hamiltonian, F_{IVO} , with eigenvalue ϵ_i :

$$F_{\text{IVO}} = T_e + V_{\text{nuc}} + 2J_m - K_m + J_n + K_n. \quad (117)$$

In Eq. (117), T_e is the one-electron kinetic energy operator, V_{nuc} is the electron nuclear attraction operator and J and K are the usual Coulomb and the exchange operators, with m referring to the doubly occupied orbitals and n to the valence orbital that is being polarized. Similarly, the expression for a first-order perturbed orbital in this independent orbital approximation is

$$\varphi_{n,k}^1 = \sum_i^{\text{virtual}} \frac{\varphi_i \langle \varphi_i | \mu_k | \varphi_n \rangle}{\epsilon_i - \epsilon_n}. \quad (118)$$

It is easy to show³² that this orbital can also be constructed by diagonalizing the matrix,

$$\rho_{ij}^{n,k} = \frac{\langle \varphi_i | \mu_k | \varphi_n \rangle \langle \varphi_n | \mu_k | \varphi_j \rangle}{(\epsilon_i - \epsilon_n)(\epsilon_j - \epsilon_n)}. \quad (119)$$

$\rho^{n,k}$ is a rank one operator and thus has at most one nonzero, positive eigenvalue. The corresponding eigenvector is the polarized virtual orbital we seek. In general, three polarized orbitals will be generated for each occupied valence orbital, one orbital being generated for each component of the dipole operator. Fewer than three polarized orbitals will be obtained if the Gaussian basis set does not contain $(\ell + 1)$ and $(\ell - 1)$ angular momentum functions, where ℓ is the angular momentum of the orbital being polarized. This procedure is repeated for each occupied orbital shell and

the resulting polarized orbitals are orthogonalized. The closed-channel wave functions that are used to generate Q -space in our Kohn calculations are then constructed by singly-exciting the valence orbitals into the polarized orbital space.

The use of polarized orbitals provides a very compact representation of the total wave function; we have also found this prescription to provide a reasonable balance between the long-range and short-range interactions for a number of closed-shell targets. Figure 4 compares the total cross-sections we obtained³² for CH_4 with experiment. The experimental points in the 3–10 eV range are those of Lohman and Buckman.⁸³ The inset to Fig. 4 shows the cross-section in the vicinity of the Ramsauer-Townsend minimum along with the experimental results of Sohn *et al.*⁸⁴ The agreement is quite good. In Fig. 5, we compare the differential cross-sections we obtained at 0.5 and 3.0 eV with the results of Sohn *et al.* These were the first *ab initio* calculations on a polyatomic target to achieve this kind of accuracy.

The same kind of treatment was applied to the $e^- + \text{SiH}_4$ system with comparable success.⁷⁷ The total cross-sections are shown in Fig. 6 along

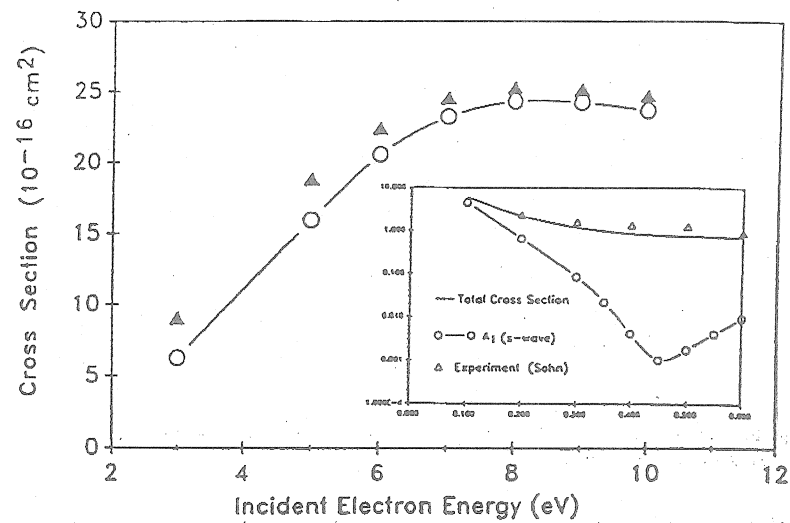


Fig. 4. Total elastic cross-sections for $e^- + \text{CH}_4$. Experimental points (triangles) are those of Sohn *et al.*⁸⁴

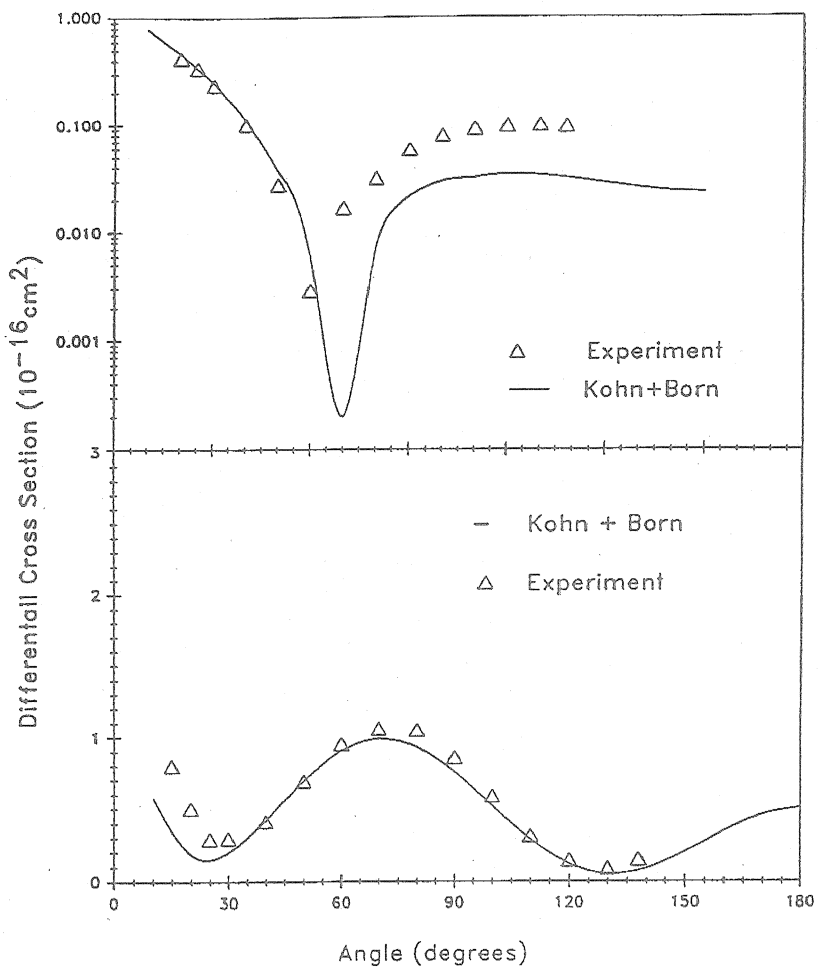


Fig. 5. Differential $e^- + \text{CH}_4$ cross-sections. Upper part, 0.5 eV; lower part, 3.0 eV. Experimental points from Ref. 84.

with the experimental results of Wan *et al.*⁸⁵ and the model potential results of Jain *et al.*⁸⁶ and Yuan.⁸⁷ The inset to Fig. 6 again shows the cross-section in the vicinity of the Ramsauer-Townsend minimum. This figure highlights a problem that is typical of model potential approaches:

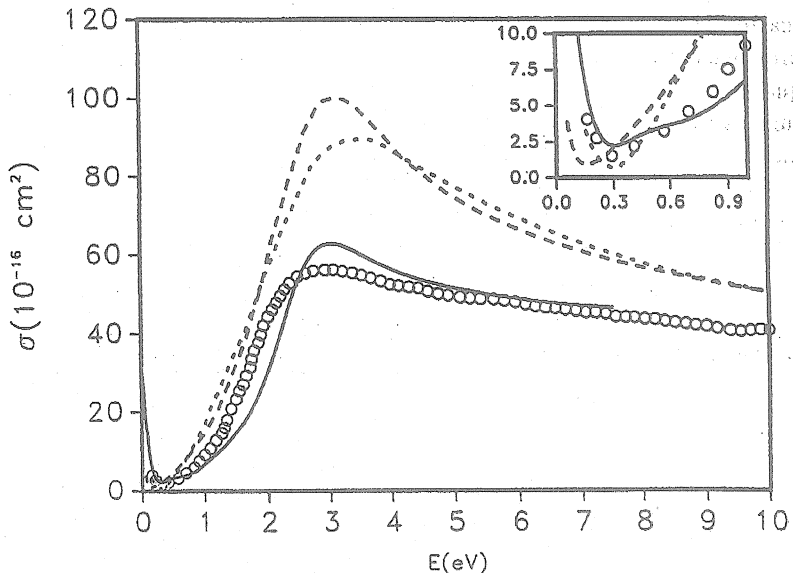


Fig. 6. Total elastic cross-sections for $e^- + \text{SiH}_4$. Solid curve, complex Kohn results; long-dashed line, model polarization results of Jain *et al.*⁸⁶; short-dashed line, model potential results of Yuan⁸⁷; circles, experimental results of Wan *et al.*⁸⁵

an adiabatic polarization potential that is designed to accurately describe the scattering in the low-energy region does not necessarily work well in describing a higher energy shape resonance. Although the complex Kohn results are, of the theoretical studies, in closest agreement with experiment, they evidently overestimate the cross-section at the resonance maximum. Discrepancies in this range are even more pronounced in the momentum transfer cross-section.⁷⁷ For a target like silane, which has low-lying unoccupied d -orbitals, the use of a SCF target wave function may not be adequate to achieve quantitative cross-sections in the vicinity of a d -wave shape resonance. In this connection, it is worth noting that our procedure for generating polarized orbitals can be generalized to MCSCF target wave functions.⁸⁸ Such techniques are routinely used in electronic structure theory to extract the dipole moment from a correlated wave function or to differentiate Born-Oppenheimer energy expressions with respect to the position of the atoms.⁸⁹

Complex Kohn calculations on low-energy electron-ethylene (C_2H_4) scattering were, significantly, the first *ab initio* calculations to confirm the presence of the Ramsauer-Townsend effect in a molecule with a permanent quadrupole moment.⁷⁸ Although there was some experimental evidence to suggest this finding,⁹⁰ there was also considerable reluctance among experimentalists in accepting this data as fact.

We have also carried out both static-exchange and polarized-SCF calculations for the electron-ethane (C_2H_6) system.⁷⁶ Figure 7 shows that the polarized-SCF total cross-sections for staggered C_2H_6 agree very well with the most recent experimental results,^{91,92} especially at energies below 3.0 eV. The inclusion of target polarization and orbital relaxation is evidently essential if one is to generate reliable cross-sections in the vicinity

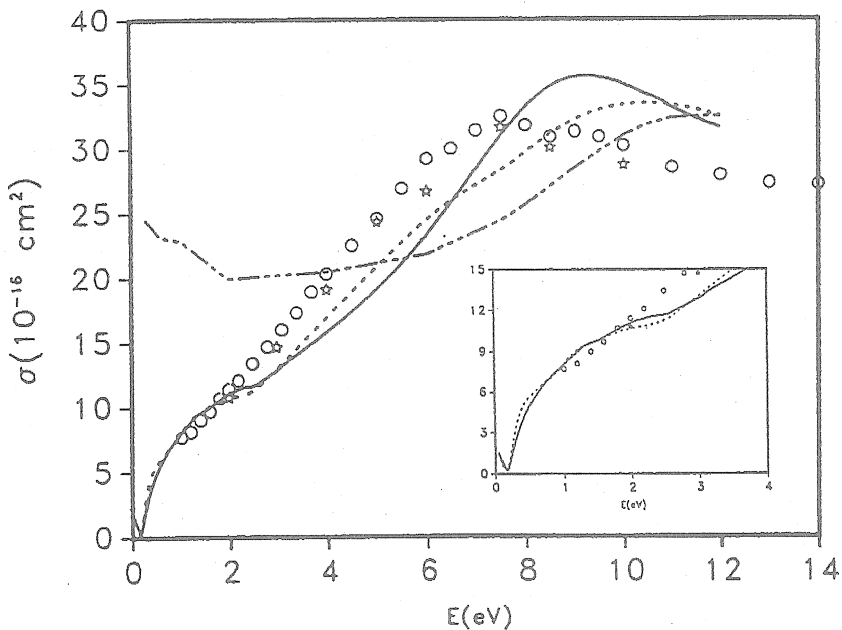


Fig. 7. Total elastic cross-sections for $e^- + C_2H_6$. Solid curve, polarized-SCF results for staggered ethane; dotted line, polarized-SCF results for eclipsed ethane; dash-dotted line, static-exchange results for staggered ethane. Experimental points from Ref. 91 (circles) and Ref. 92 (stars).

of the RT minimum and the *f*-wave shape resonance. The static-exchange results fail to show the correct low-energy behavior of the integral cross-section and place the resonance at too high an energy. With the polarized-SCF results, we see that the *f*-wave shape resonance in the eclipsed conformer is found at higher energy than the resonance in the staggered conformer. At the static-exchange level, the staggered and eclipsed conformers give similar cross-sections. The polarized-SCF results confirmed the shift in the position of the RT minimum from CH_4 (0.45 eV) to C_2H_6 (0.18 eV) found by Christophorou and McCorkle.⁹³ Figures 8 and 9 show the calculated differential cross-sections at 4.0 and 6.0 eV, respectively, along with the experimental results of Tanaka *et al.*⁹² The failure of the static-exchange model to produce the observed structure in the DCS is especially evident from these figures, whereas the agreement between the polarized-SCF results and experiment is good.

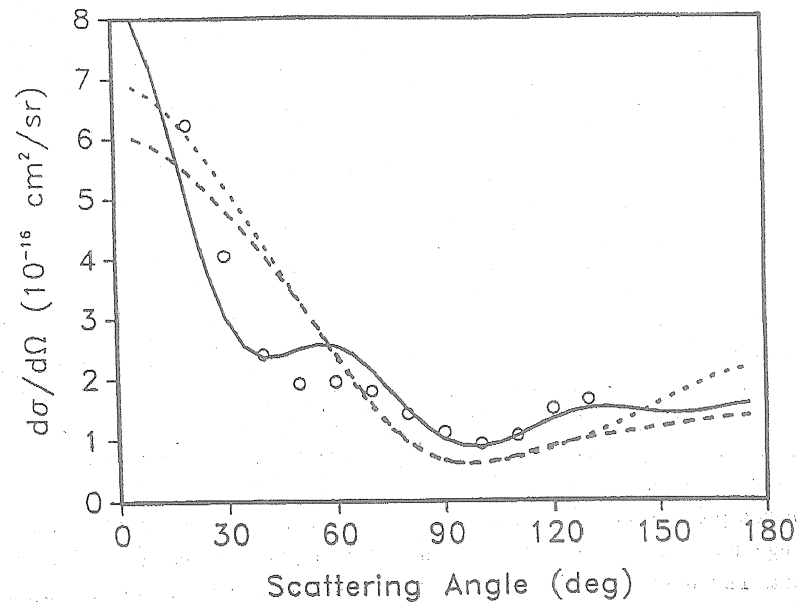


Fig. 8. $e^- + C_2H_6$ differential cross-sections at 4 eV. Solid curve, polarized-SCF result for staggered ethane; short-dashed curve, static-exchange results for eclipsed ethane; long-dashed curve, static-exchange results for staggered ethane; circles, experimental results from Ref. 92.

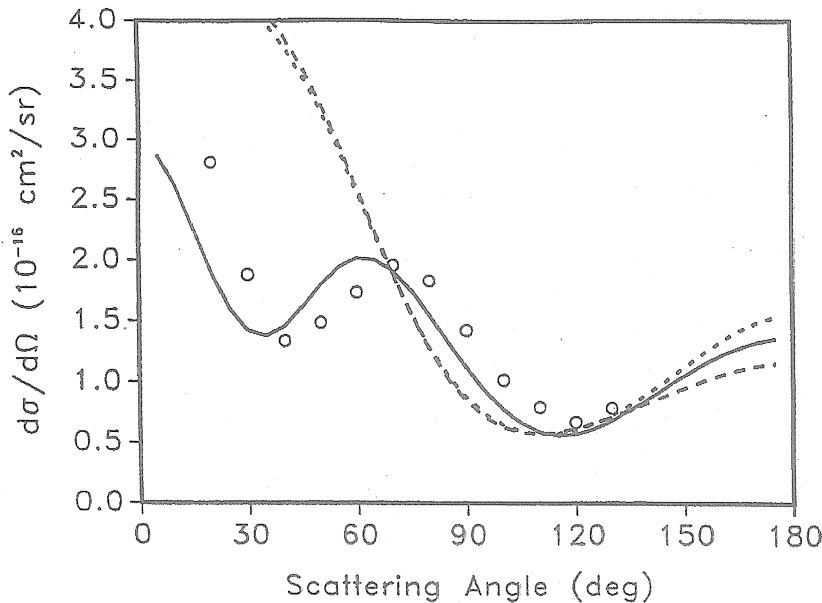


Fig. 9. As in Fig. 8, for 6 eV.

5.2. Polar Molecules (H_2O , NH_3 and H_2S)

We have already pointed out that many aspects of low-energy electron scattering by polar molecules are largely determined by the underlying electron-dipole interaction. The fact that many partial waves are required for convergence and that the Born approximation proves adequate for all but the lowest partial-wave contributions leads one to suspect that polarization effects may not be nearly as important in these systems as they are for non-polar targets. It turns out that there is a relatively narrow energy range above a few electron volts where target polarization can be important. The magnitude of the effect depends on the relative size of the target polarizability and its dipole moment. Below this range, the Born approximation is generally valid. Above this range, where the incident electron can penetrate the target, the static-exchange approximation is adequate for evaluating the elastic cross-sections.

We have carried out variational calculations for elastic scattering of electrons by H_2O , NH_3 and H_2S (Refs. 73, 66 and 94 respectively) using single-configuration SCF target wave functions. The scattering calculations were undertaken at both the static-exchange and polarized-SCF levels. The basis sets for both oxygen and nitrogen consisted of Dunning's⁹⁵ [5s 3p] contraction of a (9s 5p) Gaussian basis, augmented with two additional s- and p-type functions and four additional d-type functions. For sulfur, we used McLean and Chandler's⁹⁶ [6s 5p] contraction of a (12s 9p) basis, augmented with three s-, three p- and five d-type functions. The hydrogen basis in all cases was Dunning's (4s)/[3s] basis with one p-type function. The dipole moments and polarizabilities from our SCF and single-excitation CI calculations, respectively, are compared with experimental values in Table 1.⁹⁷⁻⁹⁹ Judging from the magnitude of the polarizabilities and dipole moments, we would expect H_2S to show the most sensitivity to the inclusion of target polarization.

Table 1. First-order properties of H_2O , NH_3 and H_2S .

Molecule	Dipole Moment (a.u.)		Polarizability, $\alpha_0(\text{a}^3_0)$	
	SCF	Experiment	Singles-CI	Experiment
H_2O	0.781	0.724	9.51	9.82
NH_3	0.633	0.579	14.43	14.82
H_2S	0.432	0.386	28.2	24.8

In Figs. 10-12, we show elastic differential cross-sections for H_2O , NH_3 and H_2S at three different energies. The experimental values for these three systems are those of Danjo and Nishimura,¹⁰⁰ Alle et al.¹⁰¹ and Buckman,¹⁰² respectively. The static-exchange and polarized-SCF results were obtained using Born closure, as outlined in Sec. 4.1. The Born approximation gives cross-sections that drop off monotonically with increasing angle. We see in all three cases that the cross-sections develop a significant backward peak as the energy increases, indicating a significant deviation from the Born approximation. The effect is most pronounced in H_2S , as expected, which shows significant non-Born behavior, even at 2 eV. Figures 13 and 14 show the momentum transfer cross-sections for H_2O and NH_3 .

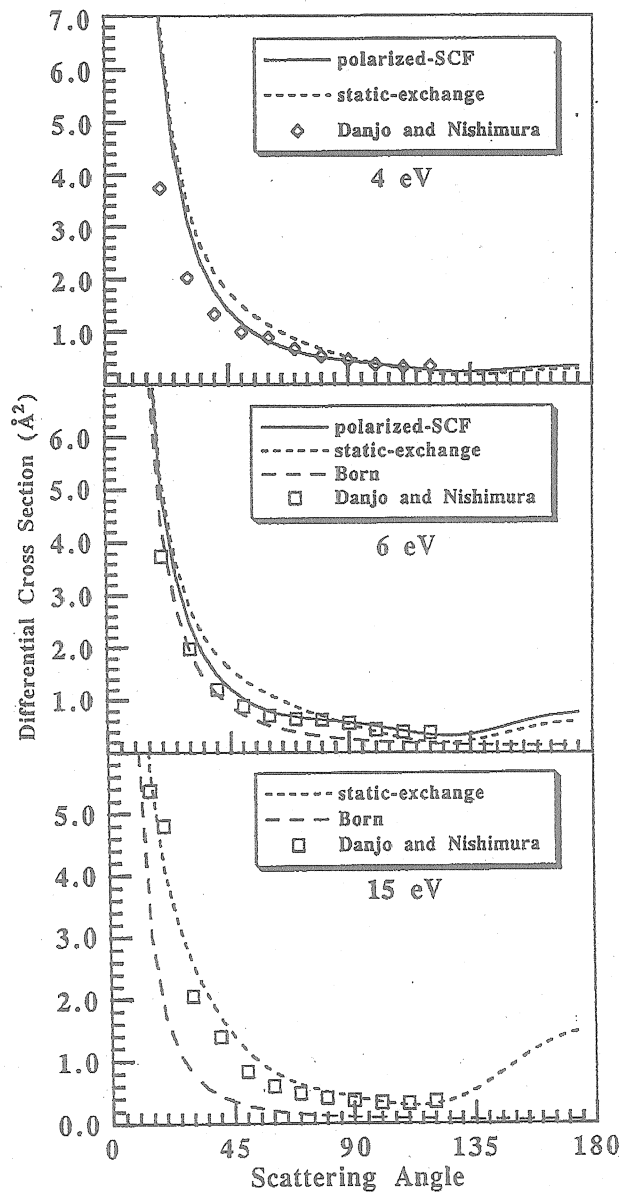


Fig. 10. Differential cross-sections for $e^- + \text{H}_2\text{O}$. Experimental points from Ref. 100.

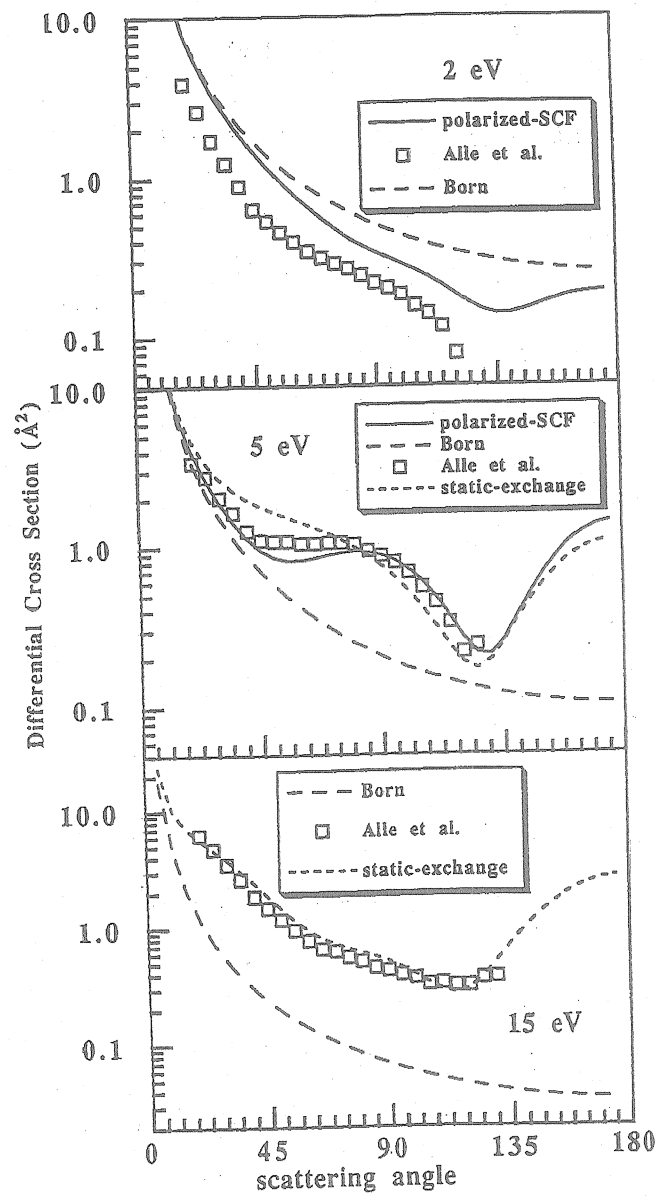


Fig. 11. Differential cross-sections for $e^- + \text{NH}_3$. Experimental points from Ref. 101.

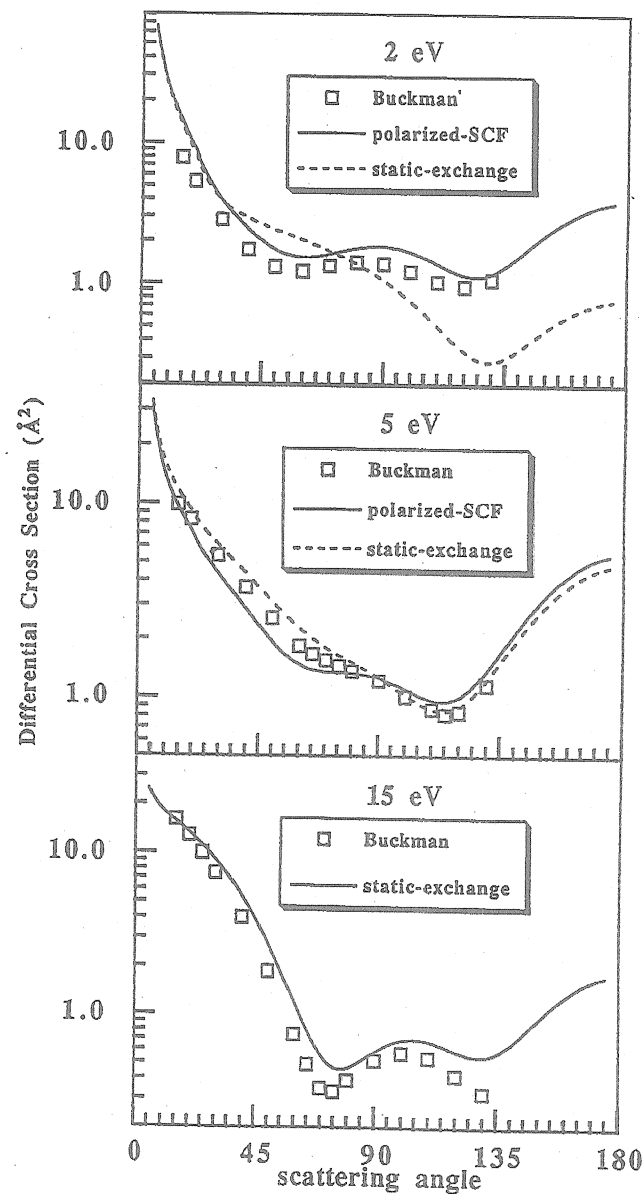


Fig. 12. Differential cross-sections for $e^- + \text{H}_2\text{S}$. Experimental points from Ref. 102.

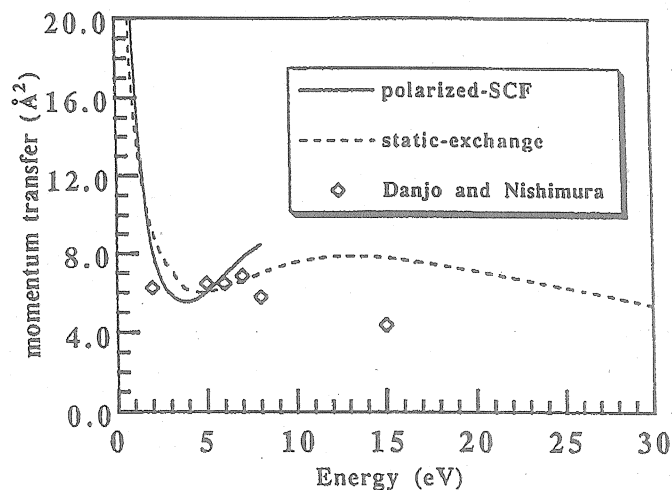


Fig. 13. Momentum transfer cross-sections for $e^- + \text{H}_2\text{O}$. Experimental points from Ref. 100.

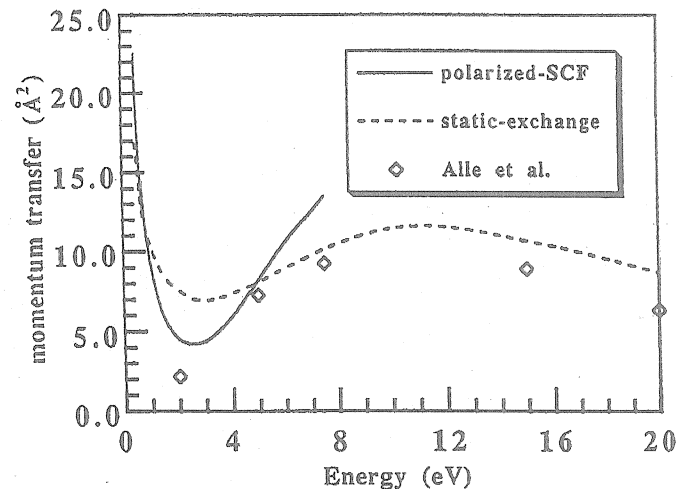


Fig. 14. Momentum transfer cross-sections for $e^- + \text{NH}_3$. Experimental points from Ref. 101.

The momentum transfer cross-section is not sensitive to the form of the differential cross-section at small angles and thus is a sensitive measure of the importance of non-Born effects. The minimum in the momentum transfer cross-section gives an indication of the energy above which the Born approximation is inadequate. This occurs at a lower energy for NH₃ than it does for H₂O. Moreover, the value of the cross-section near the minimum is more sensitive to the inclusion of polarization in NH₃ than it is in the case of H₂O.

5.3. Target Correlation Effects — The Li₂ Example

The polarized-SCF model was seen to provide a consistent balance between the N - and ($N + 1$)-electron portions of the scattering problem in systems whose ground-states are reasonably well described by a simple SCF wave function. We now turn our attention to a system where target correlation plays a dominant role — the Li₂ molecule.

The lithium dimer is an unusual molecule. It is a spatially large and weakly bound system with an equilibrium bond length of 5.05 a_0 and a dissociation energy of about 1 eV.¹⁰³ Its ionization potential is predicted to be ~ 0.5 eV, signifying a larger than usual spatial extent of the electronic wave function. In addition, Li₂ has the largest known static polarizability, $229\ a_0^3$, as well as the largest elastic low-energy electron scattering cross-section ever observed for a nonpolar molecule.¹⁰⁴ Previous theoretical work on $e^- + \text{Li}_2$ scattering included the results of Padial,¹⁰⁵ who used a model polarization potential, and the work of Schneider and Collins,¹⁰⁶ who report static-exchange and optical potential cross-sections. The results of Padial and Schneider and Collins have very little in common with each other except that they both found a very large Σ_g cross-section below 0.5 eV. In addition to these scattering calculations, there was a theoretical study of negative ion states by Michels, Hobbs and Wright.¹⁰⁷ In addition to confirming the stability of Li₂⁻ in $^2\Sigma_u^+$ symmetry, they also predicted a rich resonant structure in the electron scattering cross-sections below 1 eV; in particular, they predicted a sharp Feshbach resonance near 0.34 eV in $^2\Sigma_g^+$ symmetry and a low-energy shape resonance in $^2\Pi_u$ symmetry.

There are a number of features in the $e^- + \text{Li}_2$ elastic scattering cross-sections below 1 eV whose quantitative description depends on a delicate balance of correlation in the N - and ($N + 1$)-electron systems. We have mentioned that the Li₂⁻ anion is bound in $^2\Sigma_u^+$ symmetry, a fact that has

important implications for the scattering in that symmetry. The Li₂⁻ anion, on the other hand, is predicted to be unbound in $^2\Pi_u$ symmetry, but might be expected to show up as a resonance feature in the scattering cross-section. This was indeed the case with the model potential calculations of Padial,¹⁰⁵ which showed a $^2\Pi_u$ resonance very close to the elastic threshold. Another striking feature is the rapid rise in the $^2\Sigma_g^+$ component of the cross-section below 0.3 eV that was seen both by Padial and by Schneider and Collins in the latter's optical potential calculations. All of these features are sensitive to electron-target distortion and polarization. As a result of the importance of polarization and orbital relaxation effects, the static-exchange approximation gives a qualitatively incorrect picture of the low-energy scattering.

In a recent study,⁵⁶ we reported a series of calculations on the $e^- + \text{Li}_2$ system that used increasingly more elaborate trial wave functions. Figure 15 shows the static-exchange cross-sections from that study. By definition, this trial scattering wave function does not contain the closed channels needed to account for target response. For comparison, we have also plotted the static-exchange results of Schneider and Collins,¹⁰⁶ which were obtained with the linear-algebraic method. The agreement between the two calculations is good. The static-exchange cross-sections are dominated by a low-energy shape resonance in $^2\Sigma_u^+$ symmetry, resulting from what should be a bound negative ion. This state is pushed into the continuum when the total wave function is built from an undistorted single-configuration target state. In $^2\Pi_u$ symmetry, there is evidence of a broad shape resonance near 1 eV.

We also performed calculations with correlated target wave functions.⁵⁶ In order to test the sensitivity of our cross-sections to the way in which the target space orbitals were chosen, we performed the calculation two different ways. We first performed a single- and double-excitation valence CI on Li₂. With a view toward finding a compact set of "target" orbitals to use in the scattering calculations, we diagonalized the ground-state one-electron density matrix and extracted the seven natural orbitals with the largest occupation numbers. This included three σ_g orbitals, two σ_u orbitals and a set of π_u orbitals. We carried out complex Kohn calculations using the electron distributions given in Table 2. The first distribution generates the P -space corresponding to the direct product of the ground-state wave function and an additional electron in a subspace of orbitals orthogonal to the

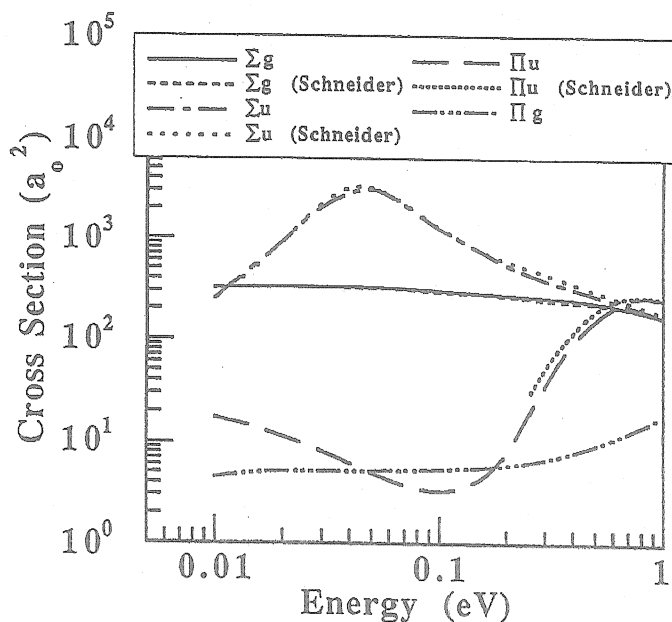


Fig. 15. $e^- + \text{Li}_2$ cross-sections in the static-exchange approximation. Comparison of complex Kohn results with those of Ref. 106.

natural orbitals. The first distribution also generates Q -space terms corresponding to the direct products obtained from a scattering orbital and all of the N -electron eigenstates, other than the ground-state, that can be constructed from the natural orbitals. The second distribution completes the Q -space contributions arising from closed-channels by including direct products of a scattering orbital with target states obtained by single-excitations from the natural orbital space. The third distribution, which generates $(N+1)$ -electron penetration terms where all electrons occupy natural orbitals, relaxes any orthogonality constraints placed on the total wave function.

We also performed calculations in a molecular orbital basis that gives an average description of the low-lying states of the target and is not biased toward the ground-state. We performed single- and double-excitation valence CI calculations and extracted the seven lowest eigenvalues and

eigenvectors. An average one-electron density was formed for these seven states by summing the density matrices of individual CI roots. The average natural orbitals were computed as eigenvectors of the average density. We kept the 15 orbitals with the highest occupation numbers, since we found that the excitation energies to the low-lying states, as well as the polarizability, were all well described by CI calculations performed exclusively in this natural orbital space. Therefore, we built the Kohn trial function for this set of calculations from only two classes of electron distributions (see Table 2), omitting the class that we had used with the smaller natural orbital set corresponding to single excitations out of the target space. The set of scattering orbitals is, by construction, orthogonal to the set of target natural orbitals. Thus, as the natural orbital set is expanded, the set of scattering orbitals grows correspondingly smaller and the number of Q -space penetration terms increases. Formally, the transfer of terms from P -space to Q -space only represents a repartitioning of the working equations which leaves the computed T -matrix elements and cross-sections unchanged. However, as we stated earlier, the optical potential is projected onto a square-integrable basis in the formulation we are currently using, so we must be sure that this basis is sufficiently flexible to accommodate the coupling between P -space and the large number of Q -space penetration terms that come from using a larger set of natural orbitals. Therefore, this final set of calculations was carried out in an extended basis obtained by augmenting the Gaussian basis used to perform the target CI calculations.

The cross-sections we obtained from the correlated trial function calculations are shown in Figs. 16 and 17. For the Σ_g , Σ_u and Π_g symmetry

Table 2. Electron distributions used to generate trial wave functions for complex Kohn calculations on $e^- + \text{Li}_2$.

Calculation	Occupied Valence	Virtual Orbitals
Static-exchange	2	1
Ground-state NO's	2	1
	1	2
	3	0
Averaged NO's	2	1
	3	0

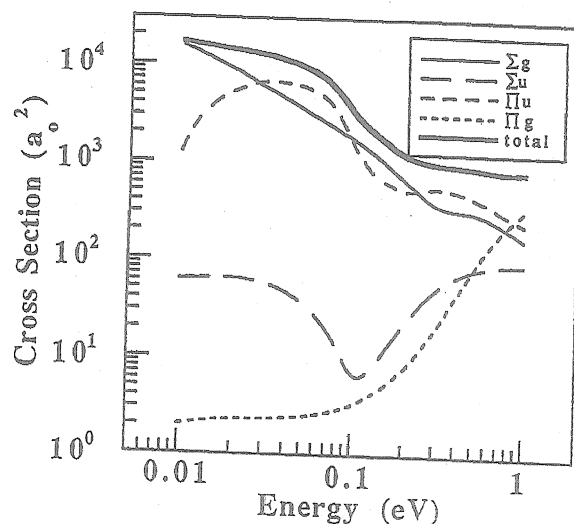


Fig. 16. $e^- + \text{Li}_2$ cross-sections using target states built from ground-state natural orbitals.

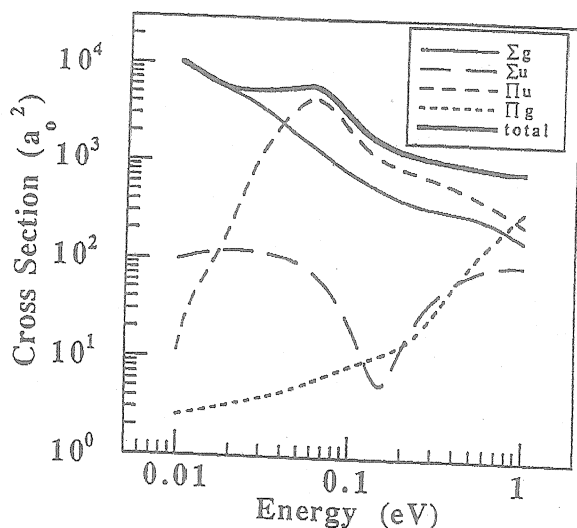


Fig. 17. $e^- + \text{Li}_2$ cross-sections using target states built from averaged natural orbitals.

contributions to the total cross-section, the two calculations give results that are reasonably close over the entire energy range considered. In contrast to the static-exchange results, the scattering is dominated by the Σ_g symmetry component at the lowest energies considered. The Σ_u cross-section shows a deep minimum near 0.1 eV. The minimum in the Σ_u cross-section component was also obtained by Padial. The Π_g component of the cross-section is evidently negligible below 0.1 eV, but begins to rise rapidly between 0.2 eV and the first inelastic threshold. While both calculations using correlated wave functions show a Π_u shape resonance, the agreement between 0.01 and 0.1 eV is only qualitative. The Π_u resonance state is effectively squeezed against the elastic threshold, and consequently the cross-section in this region is extremely sensitive to the size of the CI employed in the trial wave function.

Some of the effects seen here are also found in the corresponding electron-Li atom scattering problem.¹⁰⁸ The Li_2^- anion is electronically bound in ${}^2\Sigma_u^+$ symmetry at all internuclear separations and dissociates to $\text{Li}({}^2S) + \text{Li}({}^1S)$. The existence of this bound state evidently depletes the low-energy scattering in this symmetry, and we found what appears to be a Ramsauer-Townsend minimum near 0.1 eV in all the calculations we performed beyond the static-exchange approximation. Padial found the same feature.¹⁰⁵ The ${}^1S(e^- + \text{Li})$ cross-section is correspondingly small. The very low-energy shape resonance seen in ${}^2\Pi_u$ symmetry, which is quite sensitive to the level of correlation included in the trial wave function, is analogous to the ${}^3P^0$ resonance in $e^- + \text{Li}$ scattering which Sinfailam and Nesbet¹⁰⁸ place at 0.06 eV with a width of 0.057 eV. The large enhancement in the low energy ${}^2\Sigma_g^+$ cross-section is due to an effect which is evidently purely molecular. There is a ${}^2\Sigma_g^+$ negative ion potential curve, which also correlates with $\text{Li}({}^2S) + \text{Li}({}^1S)$ at large internuclear separations. However, unlike the ${}^2\Sigma_u^+$ curve, which remains bound, the ${}^2\Sigma_g^+$ state curve crosses the ground-state curve of the neutral molecule near 3.6 Å. This is the state that Michels *et al.*¹⁰⁷ predicted would give rise to a $2\sigma_u^2 2\sigma_g$ Feshbach resonance. However, our calculations show that what Michels *et al.* predicted to be a Feshbach resonance is in fact a virtual state. The scattering is *s*-wave dominated, and there is no temporary trapping of the incident electron in a localized state.

5.4. Electronic Excitation (H_2 , F_2 , CH_2O , C_2H_4)

An important development in electron-molecule scattering theory was the simultaneous appearance in 1985 of three *ab initio* studies on electron impact excitation of the lowest ($b^3\Sigma_u^+$) triplet state of H_2 . These three studies, using the R -matrix,¹⁰⁹ Schwinger¹¹⁰ and linear-algebraic methods¹¹¹ respectively, gave cross-sections that were in good mutual accord and agreed well with available experimental data. In one case, the two-state close-coupling studies were extended to look at excitation of the $a^3\Sigma_g^+$ ($1s2s$) and $c^3\Pi_u$ ($1s2p$) states as well, also within the two-state approximation.¹¹² However, the long-range dipole coupling between the a and c states lead us¹¹³ to question the validity of a two-state model for these excitation cross-sections. Indeed, early calculations on the excitation of the analogous $n = 2$ states of He (Ref. 114) showed that it is essential to include dipole coupling in the excited state manifold to obtain meaningful excitation cross-sections from the ground-state, since the coupling between the excited states is far stronger than the coupling between the ground and excited states.

To test this notion, we performed calculations on excitation of the first three triplet states of H_2 at incident electron energies up to 40 eV, including all three states, as well as the ground-state, in a close-coupling expansion.¹¹³ We restricted ourselves to the use of simple target wave functions, each consisting of a single configuration, and concentrated on the intermediate energy region above 13 eV where all four channels are open. The region below this energy is expected to be dominated by resonance structures that are quite sensitive to the excited singlet states we neglected.¹¹⁵ The basis sets for these calculations consisted of a large set of uncontracted (10s 10p) Gaussian functions, augmented with additional s -, p - and d -type functions, depending on the symmetry under consideration. We also included continuum functions with ℓ values up to and including six. Calculations were performed in total symmetries $^2\Sigma_g^+$, $^2\Sigma_u^+$, $^2\Pi_g$, $^2\Pi_u$, $^2\Delta_g$ and $^2\Delta_u$.

The integral cross-section for excitation of the $b^3\Sigma_u^+$ ($1\sigma_g$, $1\sigma_u$) state is relatively unchanged by coupling of the excited states, as shown in Fig. 18. This figure also shows several experimental values.¹¹⁶⁻¹¹⁸ The integral cross-sections for the $a^3\Sigma_g^+$ and $c^3\Pi_u$ states, shown in Figs. 19 and 20, show a significant change from the two-channel results.¹¹² We observe the apparent transfer of flux from the c -state to the a -state in an energy range from threshold to ~ 30 eV. There are marked differences in the relative importance of the various symmetry contributions to the cross-sections between

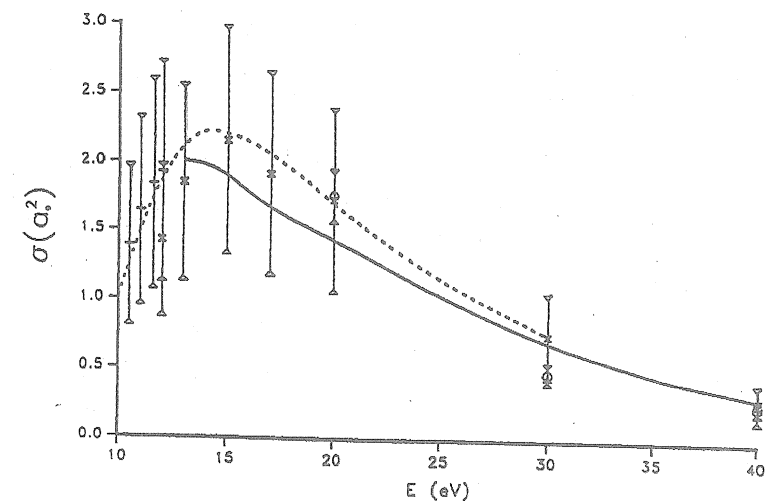


Fig. 18. Integral cross-section for the $X^1\Sigma_g^+ \rightarrow b^3\Sigma_u^+$ transition in H_2 . Solid curve, complex Kohn result; dashed curve, two-channel Schwinger result¹¹²; pluses, experiments of Nishimura and Danjo¹¹⁷; circles, experiments of Khakoo et al.¹¹⁸

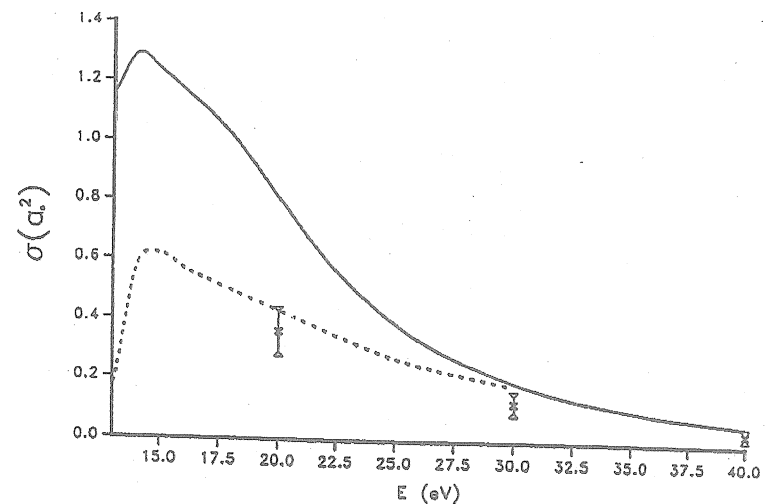


Fig. 19. As in Fig. 18, for the $X^1\Sigma_g^+ \rightarrow a^3\Sigma_g^+$ channel. The experimental points are those of Khakoo and Trajmar.¹²⁰

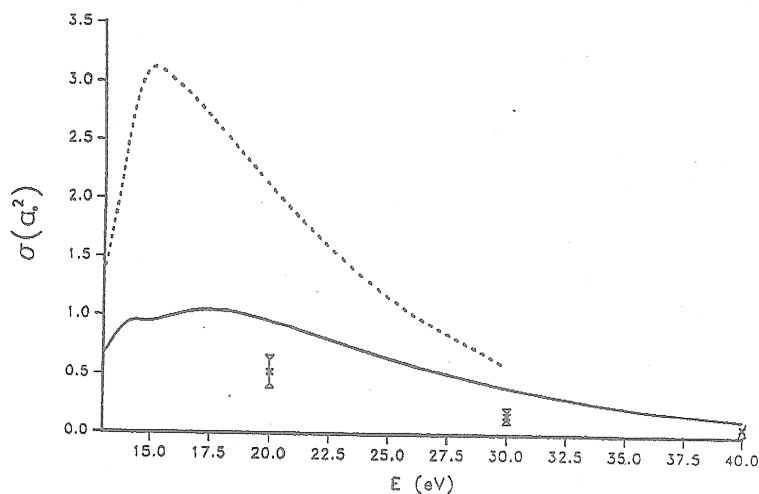


Fig. 20. As in Fig. 19, for the $X^1\Sigma_g^+ \rightarrow c^3\Pi_u$ channel.

a two-channel and a four-channel calculation. This is particularly evident in the differential cross-sections for the $a^3\Sigma_g^+$ and $c^3\Pi_u$ states, shown in Figs. 21 and 22 respectively, for an excitation energy of 30 eV. We note that the increase of the relative importance of the ${}^2\Delta_g$ contribution has a marked effect on the differential cross-section for exciting the a -state. We also note the striking similarity between our 4-channel result and the analogous 2S excitation cross-section in He (Ref. 119). We should point out that the major discrepancy between theory and experiment¹²⁰ is due to contributions from scattering near 0° and 80° , where no measurements were made. We should also point out that our theoretical findings are supported by the more extensive coupled-channel R -matrix results of Branchet and Tennyson.¹²¹

The F_2 molecule offers a considerable challenge for theoretical calculations. The electron impact dissociation cross-section for F_2 , which is important in the modeling of several laser systems (HF, KIF), turns out to be quite small and is consequently very sensitive to approximations made in the dynamics. Moreover, the total wave function used in the scattering problem should reflect the fact that the F_2^- anion is bound in ${}^2\Sigma_u^+$ symmetry.¹²² Electron-target correlation is consequently very important in the $e^- + F_2$ system.

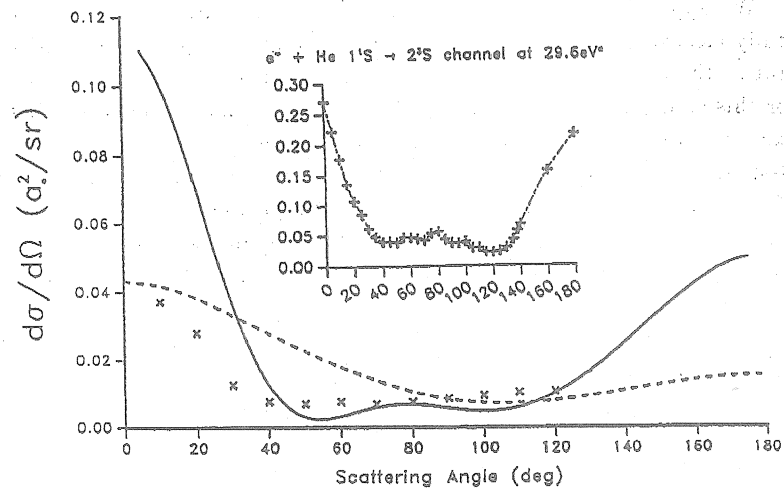


Fig. 21. Differential cross-section for excitation of $a^3\Sigma_g^+$ state of H_2 at 30 eV. Curves labeled as in Fig. 19. Inset shows excitation cross-section data for He 2S from Ref. 119.

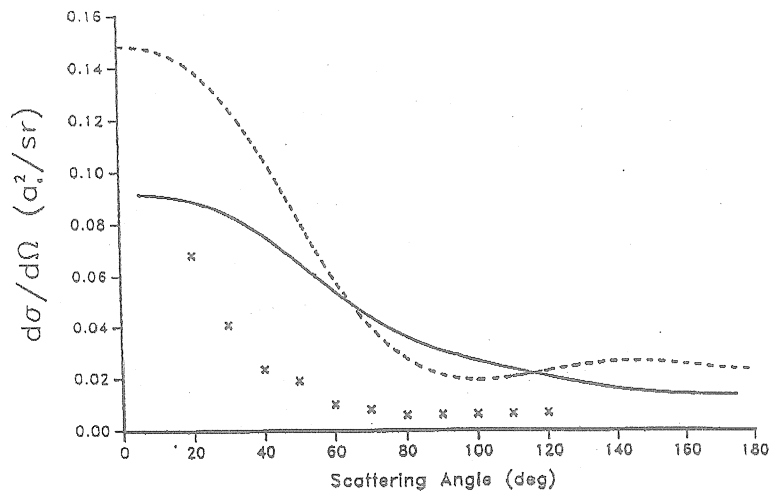


Fig. 22. As in Fig. 21, for excitation of the $c^3\Pi_u$ state at 30 eV.

We applied the intermediate energy formalism outlined in Sec. 3.3 to study electron-impact dissociation of F_2 through its two lowest electronic states, the dissociative $^3\Pi_u$ and $^1\Pi_u$ states.⁵⁷ The target wave functions for this study were obtained from CI calculations that included all single-excitations from the dominant configurations for the ground and excited Π -states. These target calculations were carried out using a truncated set of 12 natural orbits obtained from the average of the density matrices for the ground and $^1\Pi_u$ states. The excitation energies we obtained,⁵⁷ 3.28 and 4.56 eV for the $^3\Pi_u$ and $^1\Pi_u$ states respectively, agreed well with more extensive CI calculations.¹²³ We then performed three-state close-coupling calculations in an extended basis, which was obtained by augmenting the $[10s\ 7p\ 1d]$ basis used to generate the target states.

The P -space for these calculations was generated from the direct product of the three F_2 target states and the set of molecular orbitals orthogonal to the target natural orbitals. To relax the implied orthogonality constraint on the total wave function, we also included in Q -space the penetration terms generated from the direct product of the target states and the partially occupied natural orbitals. We carried out both CCPC calculations using all such Q -space terms, as well as modified MCCC calculations in which the Q -space configurations were first contracted using the scheme outlined in Sec. 3.2, and then only those ω -vectors with norms close to unity were retained in the trial wave function.

The $^2\Sigma_u^+$ component of the total wave function required special consideration, since the F_2^- ion is bound in this symmetry. Three-state MCCC calculations do not provide sufficient core relaxation to bind F_2^- and produce an artificial resonance in this symmetry.^{124,125} To remedy this deficiency, we simply determined the lowest eigenvalue of the full, uncontracted Q -space Hamiltonian and added this vector to the modified MCCC Q -space wave function. Figures 23 and 24 show the total cross-sections obtained for the $^1\Sigma_g^+ \rightarrow ^3\Pi_u$ and $^1\Sigma_g^+ \rightarrow ^1\Pi_u$ transitions using both the CCPC method and the modified MCCC technique. Evidently, the modified MCCC approach does a good job of averaging over the unphysical resonances that are evident in the CCPC cross-section. These calculations illustrate the techniques that may be necessary to obtain meaningful cross-sections over a broad range of intermediate energies in calculations that must employ correlated target wave functions. These techniques may also offer a viable alternative to the intermediate energy R -matrix theory

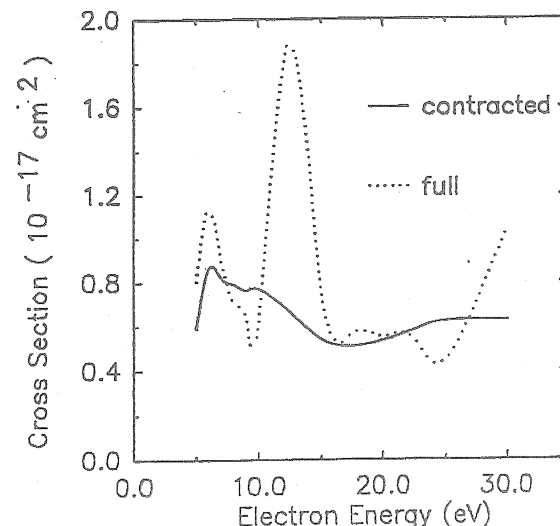


Fig. 23. Integral cross-sections for $^1\Sigma_g^+ \rightarrow ^3\Pi_u$ transition in F_2 .

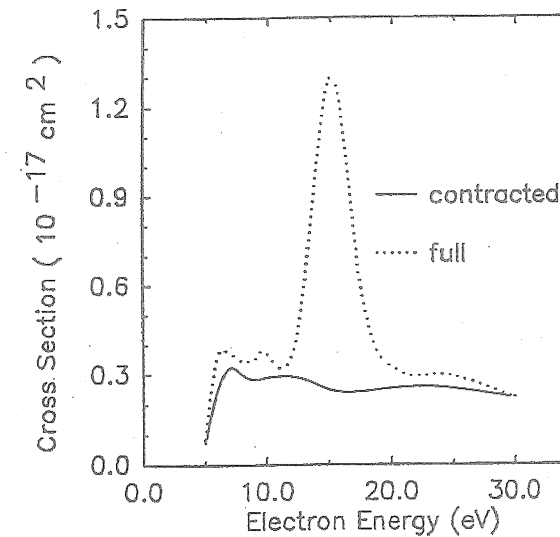


Fig. 24. Integral cross-sections for $^1\Sigma_g^+ \rightarrow ^1\Pi_u$ transition in F_2 .

proposed by Burke and coworkers,¹²⁶ in which one takes the opposite approach from that proposed here. Namely, one tries to effectively saturate the continuum by incorporating many configurations built from discretized pseudo-states.^{127,128} The idea is to make the number of pseudo-resonances in the intermediate energy region so dense that a meaningful average can be taken. This idea has only been applied to the simplest atomic systems. It is not clear whether the approach can be made practical for complicated atomic or molecular targets.

The complex Kohn calculations on the formaldehyde molecule¹²⁹ (CH_2O) constituted the first published theoretical study of electronic excitation of a polyatomic molecule by low-energy electron impact. This work was an extension of an earlier study¹³⁰ of elastic scattering on the same system which had clarified the nature of the 1 eV (2B_1) CH_2O^- shape resonance that had been observed experimentally.^{131,132} The study focused on total and differential cross-sections for exciting the two lowest ($n \rightarrow \pi^*$) ${}^1,{}^3A_2$ excited states over an energy range from 5 to 20 eV. Simple target wave functions were employed in this study. For the ground 1A_1 state, an SCF wave function was used. The excited ${}^1,{}^3A_2$ states were obtained in a frozen-core approximation by promoting the occupied $2b_2$ (oxygen lone-pair) orbital to an anti-bonding $2b_1$, (out-of-plane, π^*) orbital. We used a (9s 5p 1d) basis for both C and O contracted to [5s 3p 1d]⁹⁵ in determining the target states, along with a (4s)/[3s] hydrogen basis. The scattering calculations were performed by augmenting this basis with additional s-, p- and d-type functions on both carbon and oxygen, as well as the C–O bond center. Three-state calculations were performed in overall 2B_1 , 2B_2 , 2A_1 and 2A_2 symmetries, including continuum functions with ℓ and $|m|$ values up to 4. The only Q-space terms included in the trial wave function were the penetration terms

$$(\dots 5a_1^2 \quad 1b_1^2 \quad 1b_2^2 \quad 2b_2^2 \quad 2b_1)$$

$$(\dots 5a_1^2 \quad 1b_1^2 \quad 1b_2^2 \quad 2b_1^2 \quad 2b_2)$$

in 2B_1 and 2B_2 symmetry respectively, which are needed to relax the orthogonality of the scattering function to the $2b_1$ and $2b_2$ occupied orbitals. Figures 25 and 26 show the differential cross-sections obtained at 5 and 15 eV respectively. We found the excitation cross-sections for the 1A_2 state to be substantially smaller than those for the 3A_2 state over the entire range of energies examined. The 3A_2 cross-sections are striking in that they

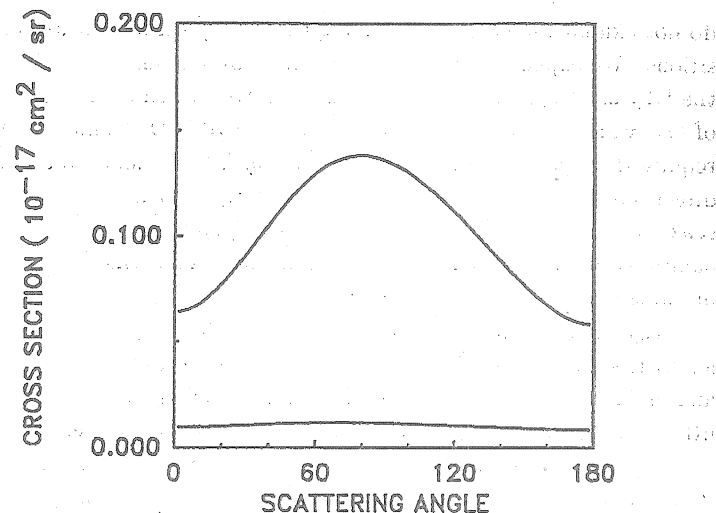


Fig. 25. Differential cross-sections for electron impact excitation of CH_2O at 5 eV. Upper curve, ${}^1A_1 \rightarrow {}^3A_2$; lower curve, ${}^1A_1 \rightarrow {}^1A_2$.

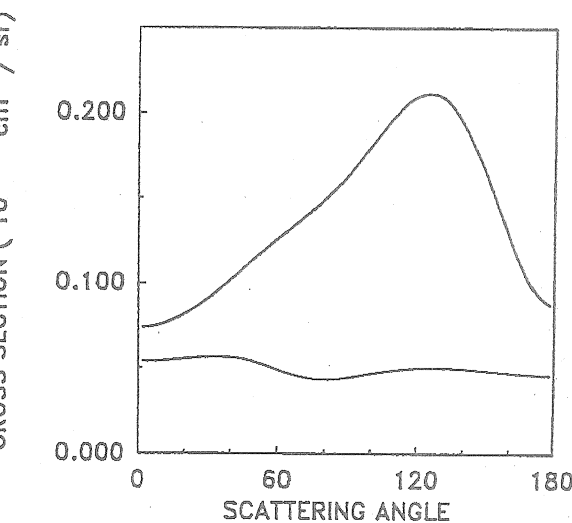


Fig. 26. As in Fig. 25, for 15 eV.

do not exhibit the backward peaking that is typical of spin-forbidden transitions. We explained this phenomenon¹²⁹ by making an analogy between the 1A_1 and 3A_2 states in CH_2O and the corresponding $^1\Sigma_g^+$ and $^3\Sigma_g^-$ states of O_2 , which is isoelectronic with formaldehyde. Diatomic selection rules require the differential cross-sections to vanish in the forward and backward directions for $\Sigma^+ \leftrightarrow \Sigma^-$ transitions.¹³³ In CH_2O , we are observing that this selection rule is quasi-preserved. We should point out that more recent calculations on this system using the Schwinger multichannel method have obtained qualitatively similar results.¹³⁴

Ethylene is important as an industrial gas and as a prototype for heavier hydrocarbons. Although useful experimental information on the total and momentum transfer cross-sections for low-energy electrons is available, little is known about electronically inelastic scattering of electrons by this molecule. The low-energy elastic scattering is notable for two reasons: a Ramsauer-Townsend minimum⁹⁰ at ~ 200 meV and a shape resonance of $^2B_{2g}$ symmetry at 1.8 eV,¹³⁵ similar in origin to the well-known π^* resonance in N_2 . We have already commented on our variational calculations which confirmed these features.⁷⁸

The experimental situation for electronically inelastic scattering in C_2H_4 is very sketchy. There have been several electron-energy-loss measurements that identify the positions of several excited states,¹³⁷ a few measurements of threshold excitation functions using the trapped electron method,^{138,139} and some relative differential cross-section experiments¹⁴⁰ that show the qualitative features expected of forbidden versus allowed electronic transitions.

Ethylene is a closed-shell molecule with a ground-state (N) of 1A_g symmetry. The first excited state ($\tilde{\alpha}$ or Mulliken's T state¹⁴¹) is of $^3B_{1u}$ symmetry, with a vertical excitation energy of 4.6 eV, while the $^1B_{1u}$ state (Milliken's V state) is located at 7.65 eV. While the ($\pi \rightarrow \pi^*$) triplet state is reasonably well characterized at the Hartree-Fock level as a valence state, the V state is more difficult to characterize because of its mixed valence-Rydberg nature. Extensive *ab initio* calculations¹⁴² have confirmed that the V state is mostly valence-like with a small Rydberg admixture. (The lowest Rydberg state of C_2H_4) is located ~ 7.1 eV above the N state.) It was our desire to obtain relatively simple representations of the excited states that preserve their essential character. This is especially important for the V state, since previous work has shown the SCF calculations pro-

duce a Rydberg-like state and that no single-configuration wave function achieves the proper valence-Rydberg balance.¹⁴³

Our approach⁷² was to start with a reasonably large orbital basis, construct CI expansions that reproduce the major correlation effects in the ground and excited states, and then use natural orbital techniques to drastically reduce the orbital space needed to reproduce the CI energies and wave functions. This enables us to achieve a compact representation of the target states for the variational scattering calculations. The target basis consisted of Dunning's (9s 5p) carbon basis⁹⁵ contracted to [4s 2p] and Dunning's (5s)/[3s] basis for hydrogen.¹⁴⁴ We included a set of *d*-functions for polarization on each carbon, along with a full set of diffuse *p* and *d* functions at the center of mass and *p* functions on the hydrogens. Calculations were carried out at the equilibrium geometry of the ground state. We performed an SCF calculation on the ground state and then carried out an all-singles calculation for the excited states. McMurchie and Davidson¹⁴² have noted that such a calculation does remarkably well in describing the V state when compared to their more extensive CI calculations. We obtained natural orbitals from the average of the density matrices for the N , T and V states. In addition to the first eight natural orbitals, which correspond to those orbitals that are strongly occupied in the ground state, we retained four more NO's — a valence-like π^* (b_{2g}), a σ^* (b_{1u}), a Rydberg b_{2g} and a b_{2u} orbital. The values obtained for the excitation energies in an all-singles CI carried out in this smaller basis were 3.64 and 8.20 eV, for the $N \rightarrow T$ and $N \rightarrow V$ transitions respectively. Our value for the $N \rightarrow V$ transition moment was 1.65 a.u., compared to McMurchie and Davidson's value of 1.76, and our value for the out-of-plane extent of the V state, as measured by $\langle \psi | \sum_i x_i^2 | \psi \rangle$, was 14.3 a.u., compared to McMurchie and Davidson's best value of 17.8.

For the scattering calculations, the target basis was augmented with additional tight as well as diffuse functions. Details can be found elsewhere.⁷² Finally, we included continuum basis functions up to $\ell = 5$, $|m| = 4$ in our calculation. Because the V state is an allowed optical transition from the ground state, many partial waves are required to obtain converged excitation cross-sections. We thus used the closure technique described in Sec. 4.1 to accelerate convergence in this case. We found the Born connections to be quite important at energies above 12 eV, accounting for $\sim 30\%$ of the total cross-section at 20 eV.

We carried out three-channel calculations over the energy range from 9 to 20 eV, where the N , T and V states are all energetically open. The only Q -space terms included in the trial function were the penetration terms generated from the dominant configuration in each target state. These terms are generated by constructing the direct products between the target natural orbitals and the three configurations $\dots \pi^2(^1A_g)$, $\dots \pi\pi^*(^3B_{1u})$, and $\dots \pi\pi^*(^1B_{1u})$, and retaining those terms consistent with the Pauli principle. This simple approach avoids the intermediate energy pseudo-resonance problem which, as we have seen, can cause unphysical behavior in the cross-sections unless special projection techniques are employed.⁵⁷ In the energy range from 4 to 8 eV, where only the N and T states are energetically open, we performed two-state calculations and included additional correlation terms to incorporate closed-channel effects. In this case, we also included all the CI relaxation terms (see Sec. 2.3) generated by the partially occupied natural orbitals. These effects become increasingly important as the collision energy decreases.

The total cross-sections for $N \rightarrow T$ and $N \rightarrow V$ excitations are shown in Figs. 27 and 28. The $N \rightarrow T$ cross-section shows a sharp peak near 5 eV, which was also observed by VanVeen¹³⁸ in an earlier trapped-electron measurement. There have also been recent two-state theoretical calculations using the Schwinger variational method.¹⁴⁵ Those calculations show a shoulder in the excitation cross-section near threshold, although the feature is less prominent than what we find. The differential cross-sections for the $N \rightarrow T$ transition, shown in Figs. 29 and 30, show that in the vicinity of the threshold peak (4–6 eV), there is pronounced resonance d -wave character, while the cross-section becomes backward peaked at higher energies. The Schwinger results display the same behavior. Analysis of the wave function reveals that it is the $^2B_{2g}$ symmetry component that is responsible for the threshold peak, and that this feature is actually caused by the tail of the low-energy, $\pi^2\pi^*$ elastic shape resonance. VanVeen mistakenly interpreted this feature as a core-excited $\pi(\pi^*)^2$ shape resonance.

The differential cross-sections for the $N \rightarrow V$ transition are shown in Figs. 31 and 32. Although there is some interesting structure that develops between 30° and 120° as the energy increases, we note that the cross-sections become increasingly forward peaked. This is the behavior expected of an optically allowed transition.

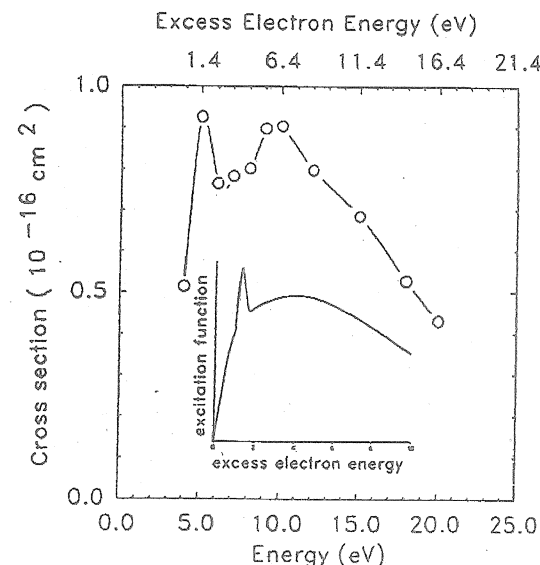


Fig. 27. Integral cross-section for $N \rightarrow T$ excitation in C_2H_4 . Inset shows $\pi \rightarrow \pi^*$ excitation function measured by VanVeen.¹³⁸

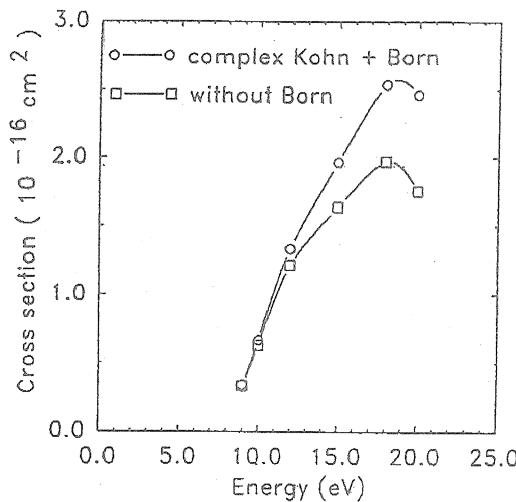


Fig. 28. Integral cross-section for $N \rightarrow V$ excitation in C_2H_4 .

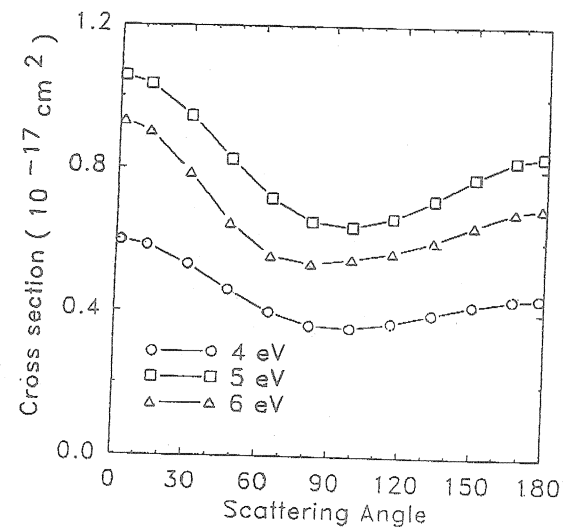


Fig. 29. Differential cross-section for $N \rightarrow T$ excitation in C_2H_4 at 4.0, 5.0 and 6.0 eV.

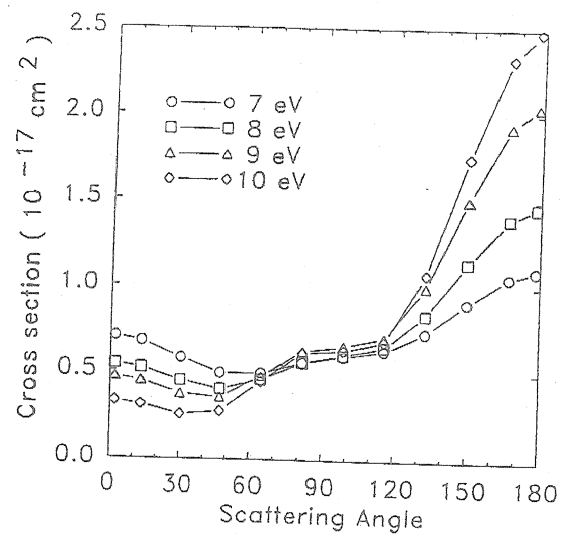


Fig. 30. As in Fig. 29, for 7.0, 8.0, 9.0 and 10.0 eV.

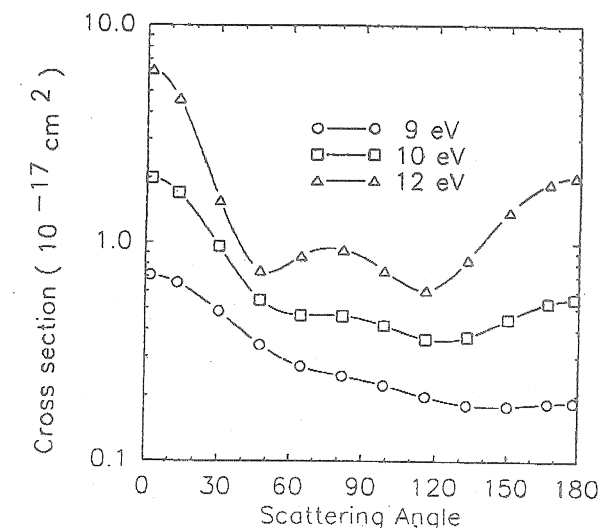


Fig. 31. Differential cross-section for $N \rightarrow V$ excitation in C_2H_4 at 9.0, 10.0 and 12.0 eV.

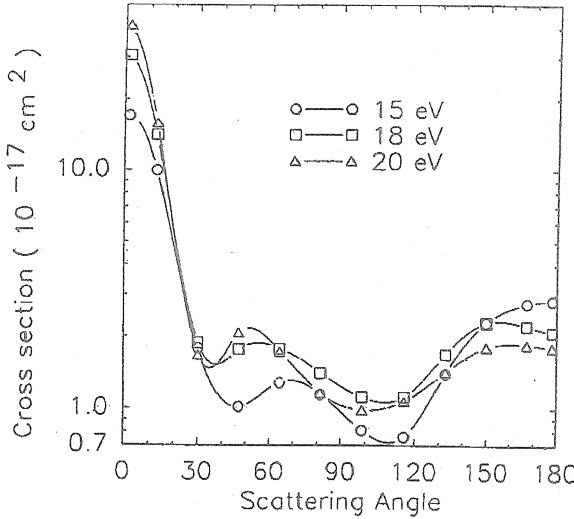


Fig. 32. As in Fig. 31, for 15.0, 18.0 and 20.0 eV.

We have focused here on electron scattering by neutral molecules. For completeness, we should also point out that the complex Kohn method has also been applied to electron impact excitation of molecular ions, notably N_2^+ , HeH^+ and H_3^+ (Refs. 31 and 60). The techniques used in those studies are entirely analogous to the methods described here. We refer the interested reader to Refs. 31 and 60 for further details.

6. Future Directions

This review has focused on the complex Kohn variational method as an efficient and flexible computational tool for studying the electron-molecule scattering problem. We have attempted to demonstrate how this method provides a general framework for incorporating modern electronic structure methodology into a difficult low-energy collision problem. This development hinges on the fact that the Kohn method is based on a Hamiltonian formulation of the collision problem, but has also benefited from a number of other theoretical developments. These include: the use of outgoing wave boundary conditions to virtually eliminate the long-standing problem of spurious numerical singularities as a matter of practical concern; the development of efficient three-dimensional adaptive quadrature techniques to compute required continuum matrix elements, thereby divorcing the method from reliance on any specific analytic schemes; the judicious use of separable approximations to transfer the major burden of the problem to the construction and manipulation of bound-bound matrix elements, where the full arsenal of bound-state structure methodology can be exploited.

Some of the methodologies discussed here have yet to be fully developed. For example, we have discussed a new technology for computing bound-free continuum matrix elements that could reduce our reliance on primitive separable approximations for representing exchange and/or optical potential interactions. This technology should enable us to drastically reduce the size of the square-integrable basis sets presently required to produce reliable cross-sections for large target molecules. Moreover, the computationally intensive evaluation of the required complex integrals is an ideal candidate for exploiting the new power of massively parallel computers.

There are also straightforward applications of the methodologies we have presented to problems other than the computation of electron collision cross-sections with neutral molecules. The variational wave functions obtained from complex Kohn calculations can easily be used to evaluate

the matrix elements needed to produce photodetachment or, with a simple change of boundary conditions, photoionization cross-sections for arbitrary polyatomic molecules, radicals or bound negative ions.¹⁴⁶

We have concentrated on a theoretical treatment of the fixed-nuclei electron-molecule problem, but we have also pointed out that many of the outstanding problems require a complimentary treatment of the nuclear dynamics. For example, an accurate treatment of threshold scattering phenomena requires a formalism that goes beyond the adiabatic nuclei approximation which underlies the development presented here. One promising method for attacking this problem is the use of an off-the-energy-shell T -matrix formalism to introduce non-adiabatic effects into the computation of rotational and/or vibrational excitation cross-sections. We have recently shown¹⁴⁷ that the complex Kohn approach can be modified to compute off-shell T -matrix elements, and have successfully applied this formalism to calculate accurate vibrational excitation cross-sections for H_2 at energies close to threshold. The real challenge for the future lies in the marriage of sophisticated *ab initio* methods for handling the electronic problem with an accurate treatment of the nuclear dynamics, which will allow investigators to probe the intimate details of electron-polyatomic molecule collisions.

Acknowledgments

This work was performed under the auspices of the US Department of Energy by the Lawrence Livermore National Laboratory under contract No. W-7405-ENG-48. CWM acknowledges support provided by the National Science Foundation under Grant No. CHE-8922836.

References

1. K. Ensslen and S. Veprek, *Plasma Chem. and Plasma Proc.* 7, 139 (1987).
2. P. Capezzuto and G. Bruno, *Pure and Appl. Chem.* 60, 633 (1988).
3. S. Veprek and M. Heintze, *Plasma Chem. and Plasma Proc.* 10, 3 (1990).
4. R. J. W. Henry and N. F. Lane, *Phys. Rev.* 183, 221 (1969).
5. P. G. Burke and A. L. SinFaiLam, *J. Phys. B3*, 641 (1970).
6. S. Chung and C. C. Lin, *Phys. Rev. A17*, 1874 (1978).
7. M. A. Morrison, N. F. Lane and L. A. Collins, *Phys. Rev. A15*, 2186 (1977).
8. L. A. Collins, W. D. Robb and M. A. Morrison, *J. Phys. B11*, L777 (1978).
9. P. G. Burke, C. J. Noble and S. Salvini, *J. Phys. B16*, L113 (1983); J. Tennyson and C. J. Noble, *ibid.* B18, 155 (1985).

10. A. W. Fliflet, in *Electron-Molecule and Photon-Molecule Collisions*, eds. T. N. Rescigno, V. McKoy and B. I. Schneider (Plenum, New York, 1979), p. 87.
11. K. Takatsuka and V. McKoy, *Phys. Rev.* **A24**, 2473 (1981); *ibid.* **A30**, 1734 (1984).
12. B. I. Schneider and L. A. Collins, *Phys. Rev.* **A33**, 2982 (1986).
13. T. Kato, *Progr. Theoret. Phys.* **6**, 394 (1951).
14. W. Kohn, *Phys. Rev.* **74**, 1763 (1948).
15. R. K. Nesbet, *Variational Methods in Electron-Atom Scattering Theory* (Plenum, New York, 1980).
16. R. K. Nesbet, *Phys. Rev.* **175**, 134 (1968); *ibid.* **179**, 60 (1969).
17. Y. Mito and M. Kamimura, *Progr. Theoret. Phys.* **56**, 583 (1976).
18. W. H. Miller and B. M. D. Jansen op de Haar, *J. Chem. Phys.* **86**, 6213 (1987).
19. C. W. McCurdy, T. N. Rescigno and B. I. Schneider, *Phys. Rev.* **A36**, 2061 (1987).
20. M. A. Morrison, *Aust. J. Phys.* **36**, 239 (1983); F. A. Gianturco and A. Jain, *Phys. Rep.* **143**, 347 (1986).
21. J. N. Bardsley, in *Electron-Molecule and Photon-Molecule Collisions*, eds. T. N. Rescigno, V. McKoy and B. I. Schneider (Plenum, New York, 1979), p. 267.
22. M. A. Morrison, *Adv. At. Molec. Phys.* **24**, 51 (1988).
23. A. U. Hazi, T. N. Rescigno and M. Kurilla, *Phys. Rev.* **A23**, 1089 (1981); A. U. Hazi, A. E. Orel and T. N. Rescigno, *Phys. Rev. Lett.* **46**, 918 (1981).
24. P. G. Burke, *Potential Scattering in Atomic Physics*, (Plenum, New York, 1977).
25. M. Abramowitz and I. A. Stegun, *Handbook of Mathematical Functions* (Dover, New York, 1965).
26. D. Lyons and R. K. Nesbet, *J. Comp. Phys.* **11**, 166 (1973); R. L. Smith and D. G. Truhlar, *Comp. Phys. Commun.* **5**, 80 (1973); J. Abdallah and D. G. Truhlar, *ibid.* **9**, 327 (1975).
27. T. N. Rescigno and A. E. Orel, *Phys. Rev.* **A43**, 1625 (1991).
28. Y. Sun, D. J. Kouri, D. G. Truhlar and D. W. Schwenke, *Phys. Rev.* **A41**, 4857 (1990).
29. See, for example, K. Gottfried, *Quantum Mechanics* (Benjamin, New York, 1966), p. 118.
30. B. I. Schneider and T. N. Rescigno, *Phys. Rev.* **A37**, 3749 (1988).
31. A. E. Orel, T. N. Rescigno and B. H. Lengsfeld III, *Phys. Rev.* **A44**, 4328 (1991).
32. B. H. Lengsfeld III, T. N. Rescigno and C. W. McCurdy, *Phys. Rev.* **A44**, 4296 (1991).
33. H. E. Saraph, M. J. Seaton and J. Shemming, *Proc. Phys. Soc. London* **89**, 27 (1966).
34. P. G. Burke, A. Hibbert and W. D. Robb, *J. Phys.* **B4**, 153 (1971).

35. H. Feshbach, *Ann. Phys. (N.Y.)* **5**, 357 (1958); *ibid.* **19**, 287 (1962).
36. B. H. Lengsfeld III and B. Liu, *J. Chem. Phys.* **75**, 478 (1981).
37. J. A. Pople, R. Krishnan, H. B. Schlegel and J. S. Binkley, *Int. J. Quantum Chem., Quantum Chem. Symp.* **13**, 225 (1979).
38. E. R. Davidson, *J. Comp. Phys.* **17**, 87 (1975); P. E. M. Siegbahn, *J. Chem. Phys.* **70**, 5391 (1980); *ibid.* **72**, 1647 (1980).
39. T. N. Rescigno and B. I. Schneider, *Phys. Rev.* **A37**, 1044 (1988).
40. T. N. Rescigno and A. E. Orel, *Phys. Rev.* **A23**, 1134 (1981); *ibid.* **24**, 1267 (1981).
41. C. W. McCurdy and T. N. Rescigno, *Phys. Rev.* **A39**, 4487 (1989).
42. See, for example, N. F. Lane, *Rev. Mod. Phys.* **52**, 29 (1980).
43. M. E. Rose, *Elementary Theory of Angular Momentum* (John Wiley, New York, 1967), pp. 62-65.
44. C. W. McCurdy and T. N. Rescigno, *Phys. Rev.* **A46**, 255 (1992).
45. This simple result is obtained by using the partial-wave decomposition of the free-particle Green's function (see Ref. 29).
46. L. I. Schiff, *Quantum Mechanics* (McGraw-Hill, New York, 1968), p. 320.
47. I. Shavitt, in *Methods in Computational Physics*, Vol. 2, eds. B. Alder, S. Fernback and M. Rottenberg (Academic, New York, 1963), p. 1.
48. L. E. McMurchie and E. R. Davidson, *J. Comput. Phys.* **26**, 218 (1978).
49. M. E. Smith, R. R. Lucchese and V. McKoy, *Phys. Rev.* **A41**, 327 (1990).
50. S. K. Adhikari and I. H. Sloan, *Phys. Rev.* **C11**, 1133 (1975).
51. K. Takatsuka, R. R. Lucchese and V. McKoy, *Phys. Rev.* **A24**, 1812 (1981).
52. W. Eissner and M. J. Seaton, *J. Phys.* **B5**, 2187 (1972).
53. R. K. Nesbet, *Comput. Phys. Comm.* **6**, 275 (1973).
54. P. G. Burke, *Comput. Phys. Comm.* **6**, 288 (1973).
55. C. Weatherford, *Phys. Rev.* **A22**, 2519 (1980).
56. T. J. Gil, C. W. McCurdy, T. N. Rescigno and B. H. Lengsfeld III, *Phys. Rev.* **A47**, 255 (1993).
57. B. H. Lengsfeld III and T. N. Rescigno, *Phys. Rev.* **A44**, 2913 (1991).
58. R. G. Newton, *Scattering Theory of Waves and Particles* (McGraw-Hill, New York, 1966), p. 432.
59. A. Messiah, *Quantum Mechanics* (North-Holland, Amsterdam, 1968), p. 839.
60. A. E. Orel, T. N. Rescigno and B. H. Lengsfeld III, *Phys. Rev.* **A42**, 5292 (1990); A. E. Orel, *ibid.* **46**, 1333 (1992).
61. O. H. Crawford and A. Dalgarno, *J. Phys.* **B4**, 494 (1971).
62. Y. Itikawa, *J. Phys. Soc. Japan* **27**, 444 (1969).
63. See, for example, L. A. Collins and D. W. Norcross, *Phys. Rev.* **A18**, 467 (1978). This paper gives a clear treatment of the subject and also contains many references to earlier work.
64. O. H. Crawford, A. Dalgarno and P. B. Hays, *Molec. Phys.* **13**, 181 (1967).
65. W. R. Garrett, *Molec. Phys.* **24**, 465 (1972).

66. T. N. Rescigno, B. H. Lengsfield III, C. W. McCurdy and S. D. Parker, *Phys. Rev.* A45, 7800 (1992).
67. See, for example, M. J. Seaton, *Proc. Phys. Soc. London* 79, 1105 (1962).
68. P. M. Chase, *Phys. Rev.* 104, 838 (1956).
69. A. M. Arthurs and A. Dalgalno, *Proc. Roy. Soc. London* A256, 540 (1960).
70. D. W. Norcross and N. T. Padial, *Phys. Rev.* A25, 226 (1982).
71. O. H. Crawford, *J. Chem. Phys.* 47, 1100 (1967).
72. T. N. Rescigno and B. I. Schneider, *Phys. Rev.* A45, 2894 (1992).
73. T. N. Rescigno and B. I. Schneider, *Z. Phys.* D24, 117 (1992).
74. I. S. Gradshteyn and I. M. Ryzhik, *Tables of Integrals, Series and Products* (Academic, New York, 1965), Eq. 7.225.3.
75. C. Ramsauer, *Ann. Physik.* 64, 513 (1921); *ibid.* 66, 546 (1921); J. S. Townsend and V. A. Bailey, *Phil. Mag.* 43, 593 (1922).
76. See, for example, H. S. W. Massey and E. H. S. Burhop, *Electronic and Ionic Impact Phenomena, Vol. I* (Oxford Univ. Press, London, 1969), p. 401.
77. W. Sun, C. W. McCurdy and B. H. Lengsfield III, *Phys. Rev.* A45, 6323 (1992).
78. B. I. Schneider, T. N. Rescigno, B. H. Lengsfield III and C. W. McCurdy, *Phys. Rev. Lett.* 66, 2728 (1991).
79. W. Sun, C. W. McCurdy and B. H. Lengsfield III, *J. Chem. Phys.* 97, 5480 (1992).
80. J. Callaway, *Phys. Rev.* 106, 868 (1957); J. Callaway, R. LaBahn, R. Pu and W. Duxler, *Phys. Rev.* 168, 12 (1968).
81. A. Temkin, *Phys. Rev.* 107, 1004 (1957); *ibid.* 116, 358 (1959); A. Temkin and J. Lamkin, *Phys. Rev.* 121, 788 (1961).
82. W. J. Hunt and W. A. Goddard III, *Chem. Phys. Lett.* 3, 414 (1969).
83. B. Lohmann and S. Buckmann, *J. Phys.* B19, 2565 (1986).
84. W. Sohn, K. H. Kochem, K. M. Scheuerlein, K. Jung and H. Ehrhardt, *J. Phys.* B19, 3625 (1986).
85. H. X. Wan, J. H. Moore and J. A. Tossell, *J. Chem. Phys.* 91, 7340 (1989).
86. A. K. Jain, A. N. Tripathi and A. Jain, *J. Phys.* B20, L389 (1987).
87. J. M. Yuan, *J. Phys.* B22, 2589 (1989).
88. M. Page, P. Saxe, G. F. Adams and B. H. Lengsfield III, *J. Chem. Phys.* 81, 434 (1984).
89. *Geometrical Derivatives of Energy Surfaces and Molecular Properties*, Vol. 166 of *NATO Advanced Study Institute, Series C: Mathematical and Physical Sciences*, eds. P. Jorgensen and J. Simons (D. Reidel, Dordrecht, 1986).
90. M. J. W. Boness, I. W. Larkin, J. B. Hasted and L. Moore, *Chem. Phys. Lett.* 1, 292 (1967).
91. O. Sueoka and S. Mori, *J. Phys.* B19, 4035 (1986).
92. H. Tanaka, L. Boesten, D. Matsunaga and T. Kudo, *J. Phys.* B21, 1255 (1988).
93. L. G. Christophorou and D. L. McCorkle, *Can. J. Chem.* 55, 1876 (1977).

94. B. H. Lengsfield III and T. N. Rescigno, unpublished results.
95. T. H. Dunning, *J. Chem. Phys.* 53, 2823 (1970).
96. A. D. McLean and G. S. Chandler, *J. Chem. Phys.* 72, 5639 (1980).
97. A. L. McClellan, *Tables of Experimental Dipole Moments* (W. H. Freeman, San Francisco, 1963).
98. H. J. Werner and W. Meyer, *Molec. Phys.* 31, 855 (1976).
99. R. L. Martin, E. R. Davidson and D. F. Eggers, *Chem. Phys.* 38, 341 (1979).
100. A. Danjo and H. Nishimura, *J. Phys. Soc. Japan* 54, 1224 (1985).
101. D. T. Alle, R. J. Gulley, S. J. Buckman and M. J. Brunger, *J. Phys.* B25, 1533 (1992).
102. S. A. Buckman, private communication.
103. D. D. Konowalow and J. L. Fish, *Chem. Phys.* 84, 463 (1984).
104. T. M. Miller, A. Kasdan and B. Bederson, *Phys. Rev.* A25, 1777 (1982).
105. N. T. Padial, *Phys. Rev.* A32, 1379 (1985).
106. B. I. Schneider and L. A. Collins, in *Wavefunctions and Mechanisms from Electron Scattering Processes*, eds. F. A. Gianturco and G. Stefani (Springer, Berlin, 1984), p. 55.
107. H. H. Michaels, R. H. Hobb and L. A. Wright, *Chem. Phys. Lett.* 118, 67 (1985).
108. A. L. SinFailLam and R. K. Nesbet, *Phys. Rev.* A7, 1987 (1973).
109. K. L. Beluga, C. J. Noble and J. Tennyson, *J. Phys.* B18, L851 (1985).
110. M. A. P. Lima, T. L. Gibson, C. C. Lin and V. McKoy, *J. Phys.* B18, L865 (1985).
111. B. I. Schneider and L. A. Collins, *J. Phys.* B18, L857 (1985).
112. M. A. P. Lima, T. L. Gibson, V. McKoy and W. M. Huo, *Phys. Rev.* A38, 4527 (1988).
113. S. A. Parker, C. W. McCurdy, T. N. Rescigno and B. H. Lengsfield III, *Phys. Rev.* A43, 3514 (1991).
114. See Ref. 76, p. 549.
115. S. E. Branchett and J. Tennyson, *Phys. Rev. Lett.* 64, 2889 (1990).
116. R. I. Hall and L. Andric, *J. Phys.* B17, 3815 (1984).
117. H. Nishimura and A. Danjo, *J. Phys. Soc. Japan* 55, 3031 (1986).
118. M. A. Khakoo, S. Trajmar, R. McAdams and T. W. Shyn, *Phys. Rev.* A35, 2832 (1987).
119. S. Trajmar, *Phys. Rev.* A8, 191 (1973).
120. M. A. Khakoo and S. Trajmar, *Phys. Rev.* A34, 146 (1986).
121. S. E. Branchett, J. Tennyson and L. A. Morgan, *J. Phys.* B23, 4625 (1990).
122. T. N. Rescigno and C. F. Bender, *J. Phys.* B9, L329 (1976).
123. D. C. Cartwright and P. J. Hay, *J. Chem. Phys.* 70, 3191 (1979).
124. B. I. Schneider and P. J. Hay, *Phys. Rev.* A18, 2049 (1976).
125. A. W. Fliflet, V. McKoy and T. N. Rescigno, *Phys. Rev.* A21, 788 (1980).
126. P. G. Burke, C. J. Noble and P. Scott, *Proc. Roy. Soc. London* A410, 289 (1987).

127. P. G. Burke, K. A. Berrington and C. V. Sukumar, *J. Phys.* **B14**, 289 (1981).
128. H. A. Slim and A. Stelbovics, *J. Phys.* **B20**, L211 (1987).
129. T. N. Rescigno, B. H. Lengsfeld III and C. W. McCurdy, *Phys. Rev.* **A41**, 2462 (1990).
130. T. N. Rescigno, C. W. McCurdy and B. I. Schneider, *Phys. Rev. Lett.* **63**, 248 (1989).
131. P. D. Burrow and J. A. Michejada, *Chem. Phys. Lett.* **42**, 223 (1976).
132. C. Benoit and R. Abouaf, *Chem. Phys. Lett.* **123**, 134 (1986).
133. D. C. Cartwright, S. Trajmar, W. Williams and D. L. Huestis, *Phys. Rev. Lett.* **27**, 704 (1971).
134. Q. Sun, C. Winstead, V. McKoy, J. S. E. Germano and M. A. P. Lima, *Phys. Rev.* **A46**, 2462 (1992).
135. P. D. Burrow and K. D. Jordan, *Chem. Phys. Lett.* **36**, 594 (1975).
136. G. Schulz, in *Principles of Laser Plasmas*, ed. G. Bekefi (Wiley-Interscience, New York, 1976), p. 33.
137. A. Kupperman and L. Raff, *J. Chem. Phys.* **37**, 2497 (1962); J. P. Doering, *J. Chem. Phys.* **46**, 2497 (1967).
138. E. H. VanVeen, *Chem. Phys. Lett.* **41**, 540 (1976).
139. H. H. Brongersma, A. J. H. Boerboom and J. Kistemaker, *Physica* **44**, 449 (1969).
140. S. Trajmar, J. K. Rice and A. Kupperman, *Adv. Chem. Phys.* **18**, 15 (1970).
141. R. S. Mulliken, *J. Chem. Phys.* **33**, 1596 (1960).
142. L. E. McMurchie and E. R. Davidson, *J. Chem. Phys.* **66**, 2959 (1977).
143. T. H. Dunning, W. J. Hunt and W. A. Goddard, *Chem. Phys. Lett.* **4**, 147 (1969).
144. T. H. Dunning, *J. Chem. Phys.* **55**, 716 (1971).
145. Q. Sun, C. Winstead, V. McKoy and M. A. P. Lima, *J. Chem. Phys.* **96**, 3531 (1992).
146. T. N. Rescigno, B. H. Lengsfeld III and A. E. Orel, *J. Chem. Phys.* **99**, 5097 (1993).
147. T. N. Rescigno, B. Elza and B. H. Lengsfeld III, *J. Phys.* **B26**, L567 (1993).

CHAPTER 10

EXACT EXPANSION METHODS FOR ATOMIC HYDROGEN IN AN EXTERNAL ELECTROSTATIC FIELD: DIVERGENT PERTURBATION SERIES, BOREL SUMMABILITY, SEMICLASSICAL APPROXIMATION, AND EXPANSION OF PHOTOIONIZATION CROSS-SECTION OVER RESONANCE EIGENVALUES

Harris J. Silverstone

*Department of Chemistry, The Johns Hopkins University,
Baltimore, Maryland 21218-2685, USA*

Contents

1. Introduction	590
2. Formal Rayleigh-Schrödinger Perturbation Theory	592
2.1. Convergence: Three Examples of RSPT for the Harmonic Oscillator	593
2.1.1. Trivial Perturbation: Linear Potential	593
2.1.2. Simple Perturbation: Change in Force Constant	594
2.1.3. Anharmonic Perturbation: Divergent RSPT	594
3. Power Series	595
3.1. Familiar Convergent Series; Convergence in a Circle	595
3.2. One Familiar Divergent Series: Stirling's Approximation	596
3.3. Standard Prototypical Asymptotic Power Series: Poincaré's Definition	596
3.4. Borel Sum of an Asymptotic Power Series	597
3.5. Complex Borel Sum of a Real Asymptotic Power Series; Stokes Line	599
3.6. Dispersion Relation and Asymptotic Power-Series Coefficients	602
4. Hydrogen Atom in Constant Electric Field	603
4.1. LoSurdo-Stark Effect	603